Identification of Power Generator Dynamics from Normal Operating Data

Lindahl, Sture; Ljung, Lennart

1972

Document Version:
Publisher's PDF, also known as Version of record

IDENTIFICATION OF POWER GENERATOR DYNAMICS FROM NORMAL OPERATING DATA

STURE LINDAHL
LENNART LJUNG

REPORT 7210 MAY 1972
LUND INSTITUTE OF TECHNOLOGY
DIVISION OF AUTOMATIC CONTROL

IDENTIFICATION OF POWER GENERATOR DYNAMICS FROM NORMAL OPERATING DATA

S. Lindahl and L. Ljung

ABSTRACT

Normal power system operating data is analyzed in order to obtain a small-signal dynamical model of a power generator. The data is analyzed using spectral analysis and maximum likelihood identification. Parameters in a first and a fifth order state space model are also estimated. The results are compared and presented in time and frequency domain. It is shown that if the transformer voltages ($d\psi_d/dt$ and $d\psi_q/dt$) are neglected, the resulting first order model cannot be fitted to the measured data. Under the same hypothesis it is possible to fit a fifth order model, describing the generator and its environment, to the data.

IDENTIFICATION OF POWER GENERATOR DYNAMICS FROM NORMAL OPERATING DATA

STURE LINDAHL AND LENNART LJUNG

TABLE OF CONTENTS:

1. INTRODUCTION

2. A SIMPLE SYNCHRONOUS GENERATOR MODEL

3. AVAILABLE DATA

4. PRELIMINARY ANALYSIS OF DATA

5. SPECTRAL ANALYSIS

6. ESTIMATION OF PARAMETERS IN A FIRST ORDER STATE SPACE MODEL

7. MAXIMUM LIKELIHOOD IDENTIFICATION

8. ESTIMATION OF PARAMETERS IN A FIFTH ORDER STATE SPACE MODEL

9. CONCLUSIONS

10. REFERENCES

1. INTRODUCTION

The improvement of load-frequency control of large interconnected systems requires among other things an accurate model for the power generator. Models for the power generator can be derived from basic physical laws and known parameters. Certain parameters which are required for such studies are not easily obtained. The damping torque is one such parameter and its actual value is important. An alternative approach is to determine models from experimental data. In this paper we apply some system identification methods to expermental data provided by K.N Stanton at Purdue University.

When carrying out an identification experiment there are many questions which arise naturally:

1) Purpose of the experiment
2) Planning of the experiment
3) Choice of identification method
4) Choice of perturbation signal
5) Choice of sampling interval

As the experiment is already performed we concentrate on the third question. The purpose of this paper is to compare the results of some system identification methods when the perturbation signal is normal system perturbations.

In section 2 we present the basic non-linear equations of the power generator and linearize them to obtain a linear model,

valid for small perturbations from an operating point. We concentrate on the transfer function $G_{M\omega}(s)$, relating torque (M) to angular frequency (ω). The available data are described in section 3.

Preliminary analysis of the data in section 4 yields some basic information on causality relations as well as material for comparison with the theoretical model. Section 5 is devoted to standard spectral analysis. Special attention is paid to pre-treatment of data.

In section 6 we try to estimate parameters in a first order model relating angular velocity to electrical torque. Only a minor part of the variations in angular velocity can be explained by the first order model. The maximum likelihood identification method is applied to the same data set and the results is presented in section 7. A straight forward application of the order test indicates that a fifth order model is appropriate. Based on these results we construct a fifth order state space model describing the power generator and its environment. In section 8 we try to estimate parameters in this model. The model can reasonably well predict angular velocity and voltage variations. On the other hand variations in active and reactive current cannot be predicted well, mainly due to the simple modeling of load variations.

2. A SIMPLE SYNCHRONOUS GENERATOR MODEL

A simplified 3-phase a-c synchronous generator is shown in Fig. 2.1. With rare exceptions, the armature winding of a synchronous generator is on the stator and the field winding is on the rotor as in Fig. 2.1. The rotor field winding and the stator armature windings are represented by windings f, r, s and t respectively. The field winding is excited by direct current and the transmission network is connected to the windings r, s and t.

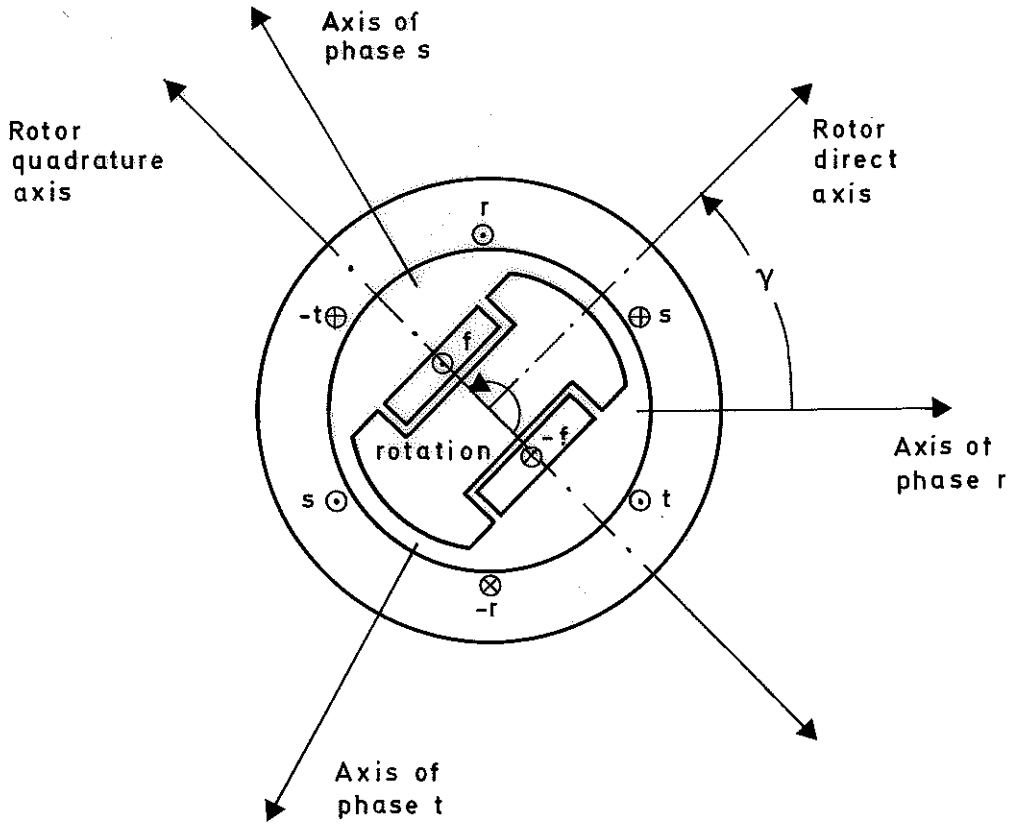

Fig. 2.1. An idealized synchronous machine

The rotor has two axes of symmetry, the polar, or direct, axis d and the interpolar, or quadrature, axis q. The magnetic flux paths have different permeances in the two axes.

For any one of the windings, in Fig. 2.1, the relation between applied voltage and input current is given by

$$v = r \cdot i + \frac{d\psi}{dt} \tag{2.1}$$

where v is the applied voltage, i the input current, r the winding resistance and ψ the flux linkage with the winding. In terms of the self- and mutual inductances, ℓ, the flux linkages are

$$\psi_r = \ell_{rr} i_r + \ell_{rs} i_s + \ell_{rt} i_t + \ell_{rf} i_f \tag{2.2}$$

$$\psi_s = \ell_{sr} i_r + \ell_{ss} i_s + \ell_{st} i_t + \ell_{sf} i_f \tag{2.3}$$

$$\psi_t = \ell_{tr} i_r + \ell_{ts} i_s + \ell_{tt} i_t + \ell_{tf} i_f \tag{2.4}$$

$$\psi_f = \ell_{fr} i_r + \ell_{fs} i_s + \ell_{ft} i_t + \ell_{ff} i_f \tag{2.5}$$

In (2.2) to (2.5) all inductances except ℓ_{ff} are functions of γ and thus time-varying. It is assumed, and can be justified [1], that the stator self- and mutual inductances have the following form

$$\ell_{xx} = \ell_{xxo} + \ell_{g2} \cos(2\gamma - \phi_{xx}) \tag{2.6}$$

$$\ell_{xy} = \ell_{xxo} + \ell_{g2} \cos(2\gamma - \phi_{xy}) \tag{2.7}$$

The stator-to-rotor mutual inductances are similarly assumed to have the form

$$\ell_{xf} = \ell_{af} \cos(\gamma - \phi_x) \tag{2.8}$$

Substituting (2.6) to (2.8) in the flux-linkage equations (2.2) to (2.5), followed by substitution of the flux-linkage expressions in the four voltage-current relations typified by (2.1), will yield a set of simultaneous equations which must be satisfied by the synchronous machine. Further analysis is greatelysimplified by a change of variables for current, voltage, and flux linkage.

The general idea underlying this change of variables is to divide the total magnetomotive force (mmf) into components along the direct and quadrature axes.

The total stator mmfs along the two axes are

$$H_d = N_a \left[i_r \cos\gamma + i_s \cos(\gamma - 2\pi/3) + i_t \cos(\gamma + 2\pi/3) \right] \tag{2.9}$$

$$H_q = N_a \left[i_r \sin\gamma - i_s \sin(\gamma - 2\pi/3) + i_t \sin(\gamma + 2\pi/3) \right] \tag{2.10}$$

We introduce new current variables i_d and i_q as

$$i_d = k_d \left[i_r \cos\gamma + i_s \cos(\gamma - 2\pi/3) + i_t \cos(\gamma + 2\pi/3) \right] \tag{2.11}$$

$$i_q = k_q \left[i_r \sin\gamma - i_s \sin(\gamma - 2\pi/3) + i_t \sin(\gamma + 2\pi/3) \right] \tag{2.12}$$

Equations (2.9) and (2.10) then simplify to

$$H_d = \frac{N_a}{k_d} \tag{2.13}$$

$$H_q = \frac{N_a}{k_q} iq \tag{2.14}$$

The same type of transformations are used for v and ψ and the resulting equations, Park's equations [2], [3], can now be written:

Flux linkage

$$\psi_f = L_f i_f - L_{af} i_d \tag{2.15}$$

$$\psi_d = L_{af} i_f - L_d i_d \tag{2.16}$$

$$\psi_q = -L_q i_q \tag{2.17}$$

Induced voltage

$$v_f = \frac{d\psi_f}{dt} + r_f i_f \tag{2.18}$$

$$v_d = \frac{d\psi_d}{dt} - r_a i_d - \omega\psi_q \tag{2.19}$$

$$v_q = \frac{d\psi_q}{dt} - r_a i_q + \omega\psi_d \tag{2.20}$$

Electrical torque at air-gap

$$M_e = \psi_d i_q - \psi_q i_d \qquad (2.21)$$

In the following it is assumed that

- The frequency error of the system can be measured as the rate of change of the angle between a fixed point on the rotor and the standard time vector. (A.2.1)

- The armature resistance of the alternator is negligible, and the energy stored in the stator is insignificant compared to that stored in the rotor. (A.2.2)

This means that all power transmitted across the air-gap is immediately available as output.

In this paper we primarily consider the equation describing the motion of the rotor:

$$J \frac{d\omega}{dt} = M_m - M_e - M_d \qquad (2.22)$$

where J is the combined moment of inertia, ω is the angular velocity of the rotor in rad/s, M_m is the mechanical torque of the prime mover, M_e the air-gap torque and M_d the damping torque.

The mechanical torque M_m can be expressed as

$$M_m = P_m/\omega \qquad (2.23)$$

where P_m is the mechanical output power from the prime mover and ω is the angular velocity of the rotor in rad/s.

For small perturbations (2.23) can be written

$$\delta M_m = \delta P_m/\omega_o - (P_m^o/\omega_o^2)\delta\omega \qquad (2.24)$$

Using assumption A2.2 it follows that (2.19) and (2.20) can be written

$$\psi_q = - v_d/\omega \qquad (2.25)$$

$$\psi_d = v_q/\omega \qquad (2.26)$$

Substituing (2.25) and (2.26) into (2.21) we have the following expression for the air-gap torque

$$M_e = (v_d i_d + v_q i_q)/\omega = V\ I_r/\omega \qquad (2.27)$$

where V is the terminal voltage of the synchronous machine, I_r is the active current both in p. u. and ω the angular velocity of the rotor in rad/s.

It is postulated that M_d in (2.22) can be written

$$M_d = D'(\omega-\omega_o) = D'\delta\omega \qquad (2.28)$$

Substituting (2.24), (2.27) and (2.28) yields

$$Jp\delta\omega = -D\delta\omega + \delta P_m/\omega_o - \delta(VI_r/\omega) \qquad (2.29)$$

where $D = D' + Pm/\omega_o^2$. When operating with blocked governor, δP_m is zero, and (2.29) becomes

$$Jp\delta\omega = - D\delta\omega - \delta M \qquad (2.30)$$

where $M = V I_r/\omega$

After Laplace-transformation we have

$$\Omega(s) = - G_M(s)M(s) \qquad (2.31)$$

where

$$G_{M\omega}(s) = \frac{1/D}{1+sJ/D} \qquad (2.32)$$

Summing up we now have: If the assumptions (A2.1) and (A2.2) are valid the transfer function $G_{M\omega}$ is of first order and given by (2.32). In section 6 we will try to fit the model to the data by adjusting the parameters D and J.

3. AVAILABLE DATA

The data available to us originate from experiments on a 50 MW, ($50\ 10^6$ watts), 0.9 PF turboalternator, reported by Stanton[4],[5].

The collection of data from a normally operating, interconnected power system is not straightforward, because the variations in observations are small relative to average operating levels. Since the identification of the power generator dynamics is based on these variations, they must be recorded with adequate resolution and without serious attenuation of rapid changes. The instrumentation used has been described elsewhere[6], and a summary of its performance is included in Table 3.1. The necessary resolution is achieved by suppressing mean levels, amplifying variations, and using digital readout.

The variables selected for measurement were:

a) the active component of armature current (I_r)
b) the reactive component of armature current (I_q)
c) the magnitude of the terminal voltage (V)
d) the power system frequency (ω)

Variable	Resolution	Errors (10min time interval)	Frequency response	Sampling rate
I_r	0.01% of I_{r0}	0.05% of I_{r0}	flat to 5c/s	8 per sec
I_q	0.02% of I_{q0}	0.05% of I_{q0}	flat to 5c/s	8 per sec
V	0.01% of V_0	0.05% of v_0	flat to 5c/s	8 per sec
ω	0.001 c/s	0.002 c/s	flat to 1c/s	2 per sec

Table 3.1. Details of instrumentation

The results described in [4] and [5] are based on four records, where "record" means a time interval of 10 to 20 minutes, during which data are collected by carefully monitoring I_r, I_q, V and ω.

Records 1, 2 and 3 were of 10 minutes duration at the sample rates indicated in Table 3.1. Record 4 was of 20 minutes duration at exactly half the sample rate of the other records. Further details are listed in Table 3.2 and it should be noted that records 3 and 4 were obtained with governor blocked.

	Operating levels					
Record	I_{r0}	I_{q0}	v_0	P_0	Q_0	Comments
	p.u.	p.u.	p.u.	MW	MVAr	
1	0.73	0.19	1.04	38	9.8	Governor normal
2	0.65	0.40	1.04	34	20.8	Governor normal
3	0.90	0.24	1.04	46.7	12.2	Governor blocked
4	0.90	0.24	1.04	46.7	12.2	Governor blocked

Table 3.2. Details of records

The machine was not subject to load-frequency control during tests, and, although the voltage regulator was connected, voltage variations were so small that they rarely exceeded the deadband of the regulator.

Records 1 and 3 were available to us and in this paper we only use Record 3 because we are interested in the open-loop dynamics.

For Record 3 we compute

a) Normalized standard deviation (r.m.s. value of variations), σ_x where

$$\sigma_x^2 = \frac{1}{N} \sum_{k=1}^{N} (X(k) - X_m)^2 / X_m^2$$

and

$$X_m = \frac{1}{N} \sum_{k=1}^{N} X(k)$$

b) Normalized max. variation, m_x where

$$m_x = \max_k |X(k) - X_m| / X_m$$

c) Normalized resolution, r_x ($r_x = R_x/\sigma_x$) where R_x is the resolution given in Table 3.1.

d) Normalized error, e_x ($e_x = E_x/\sigma_x$) where E_x is the given in Table 3.1.

The result of these computations is given i Table 3.3.

Variable	σ_x %	m_x %	r_x %	e_x %
I_r	0.32	2	4	16
I_q	1.5	8	2	4
V	0.11	0.8	10	46
ω	0.036	0.3	6	12

Table 3.3. Normalized standard deviations, max. variations, resolutions and errors.

In view of Table 3.3 we can expect difficulties when using this data for identification purpose. Although sofisticated instrumentation was used the signal-to-noise ratio (SNR) is low. Another difficulty is the absence of an artificial input signal. In Fig. 3.1 we show the measured variables from Record 3.

From the top we show frequency, voltage, active current and reactive current. The horizontal axis is graded in seconds. The scale limits are:

frequency: 49.92 - 50.1 Hz
voltage: 1.029 - 1.037 p.u
active current: 0.892 - 0.912 p.u.
reactive current: 0.220 - 0.240 p.u.

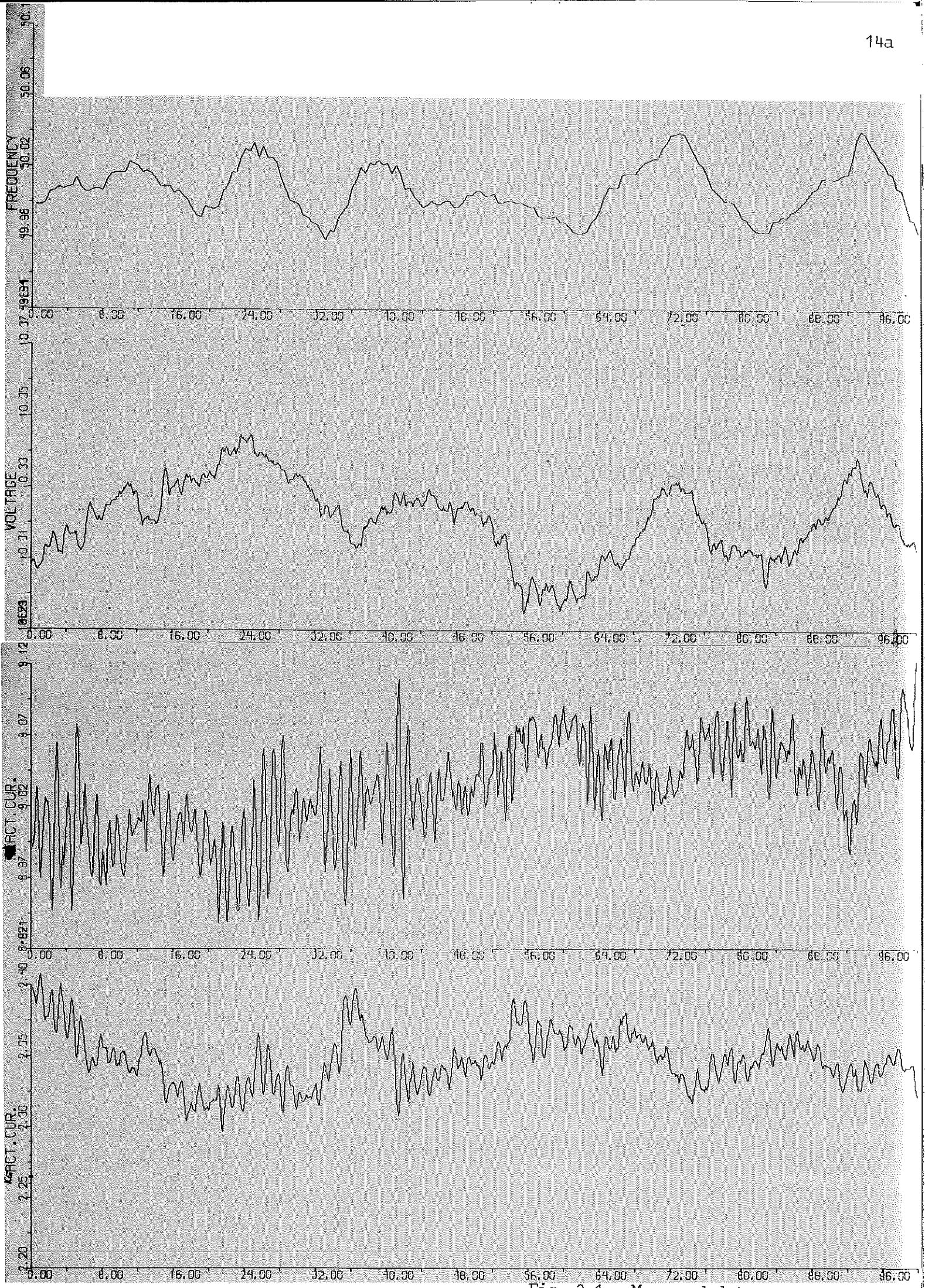

Fig. 3.1. Measured data

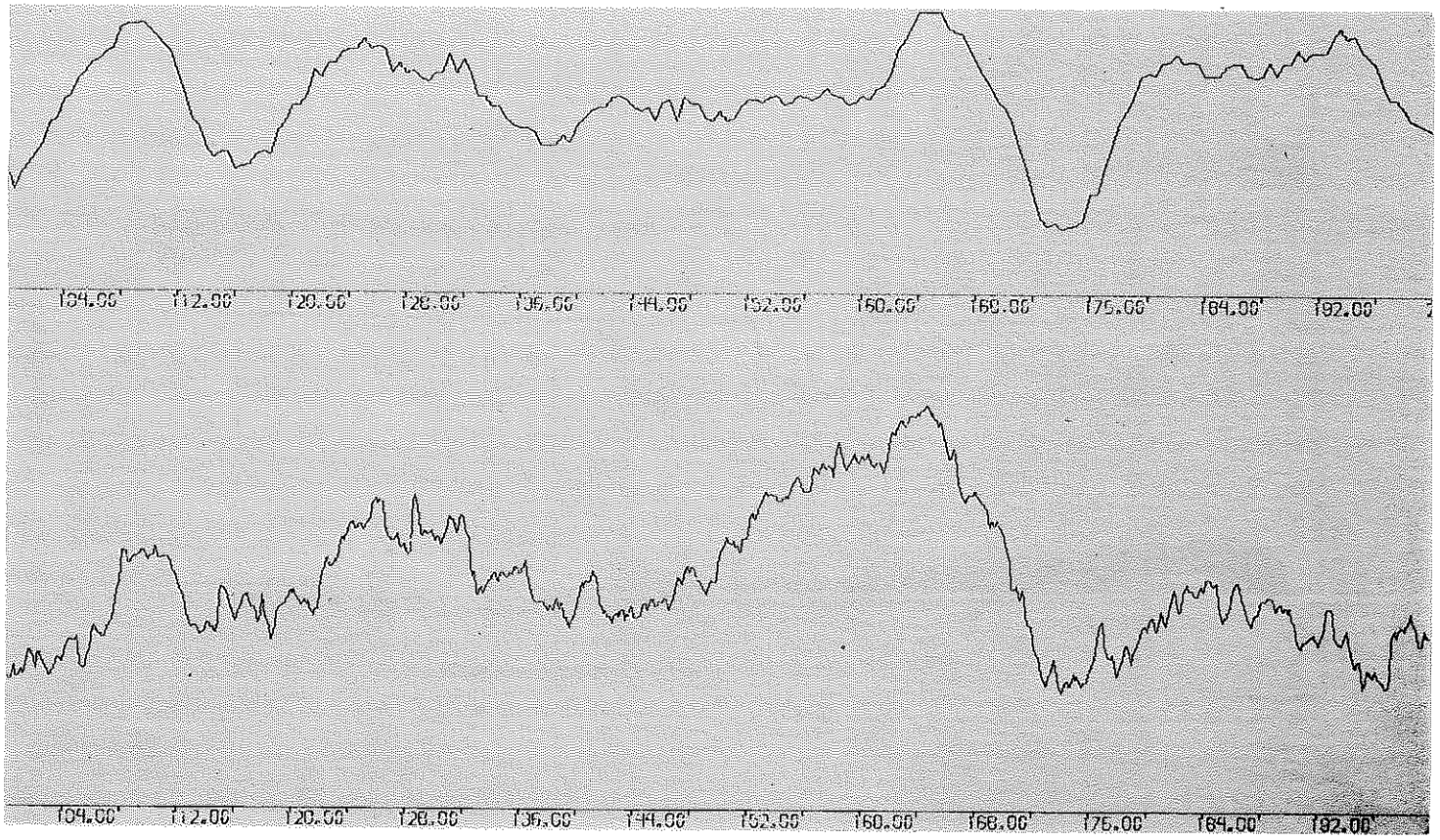
04.00'
12.00'
20.00'
28.00'
36.00'
44.00'
52.00'
60.00'
68.00'
76.00'
84.00'
92.00'

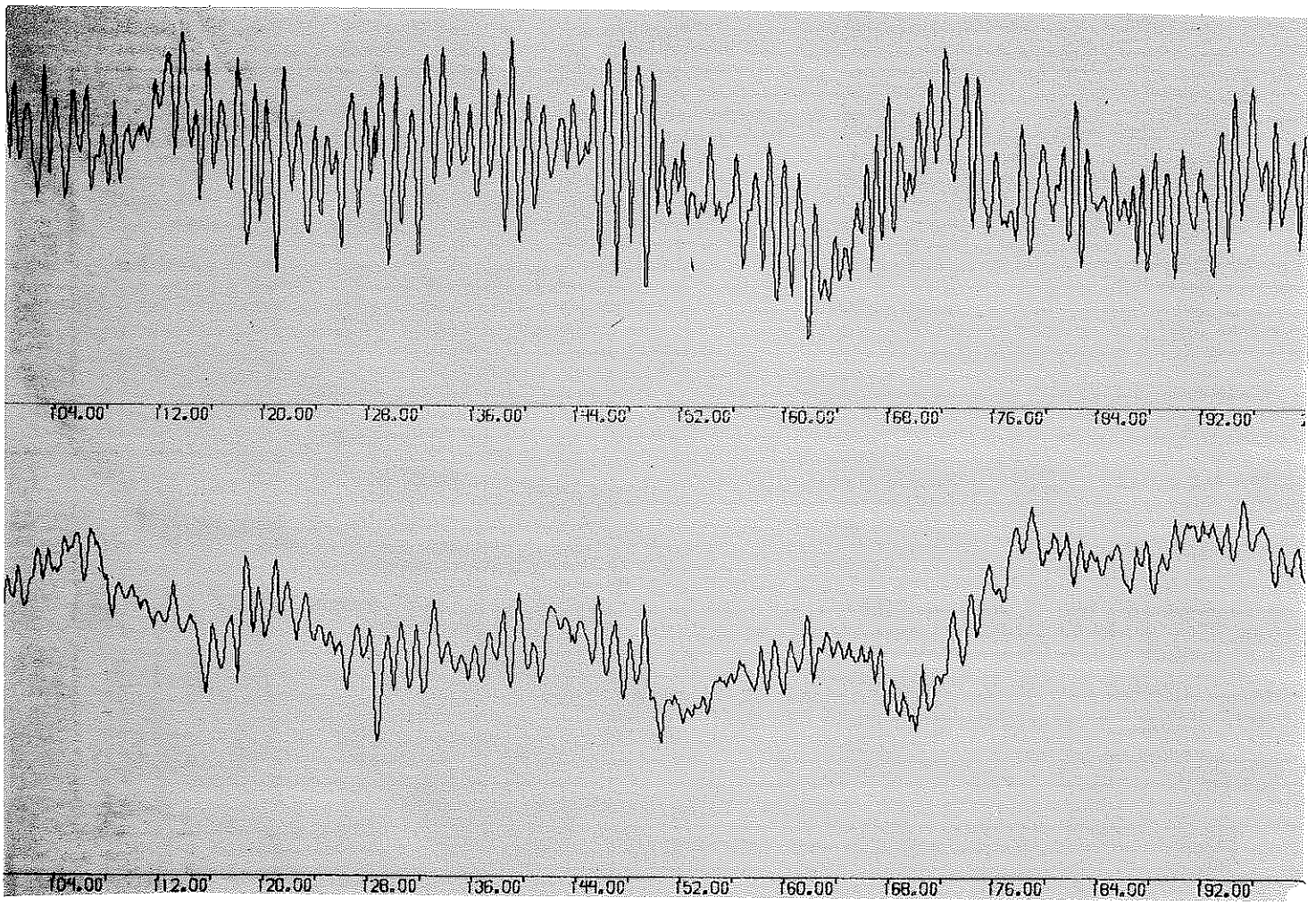
04.00'
12.00'
20.00'
28.00'
36.00'
44.00'
52.00'
60.00'
68.00'
76.00'
84.00'
92.00'

Fig. 3.1. Contd.

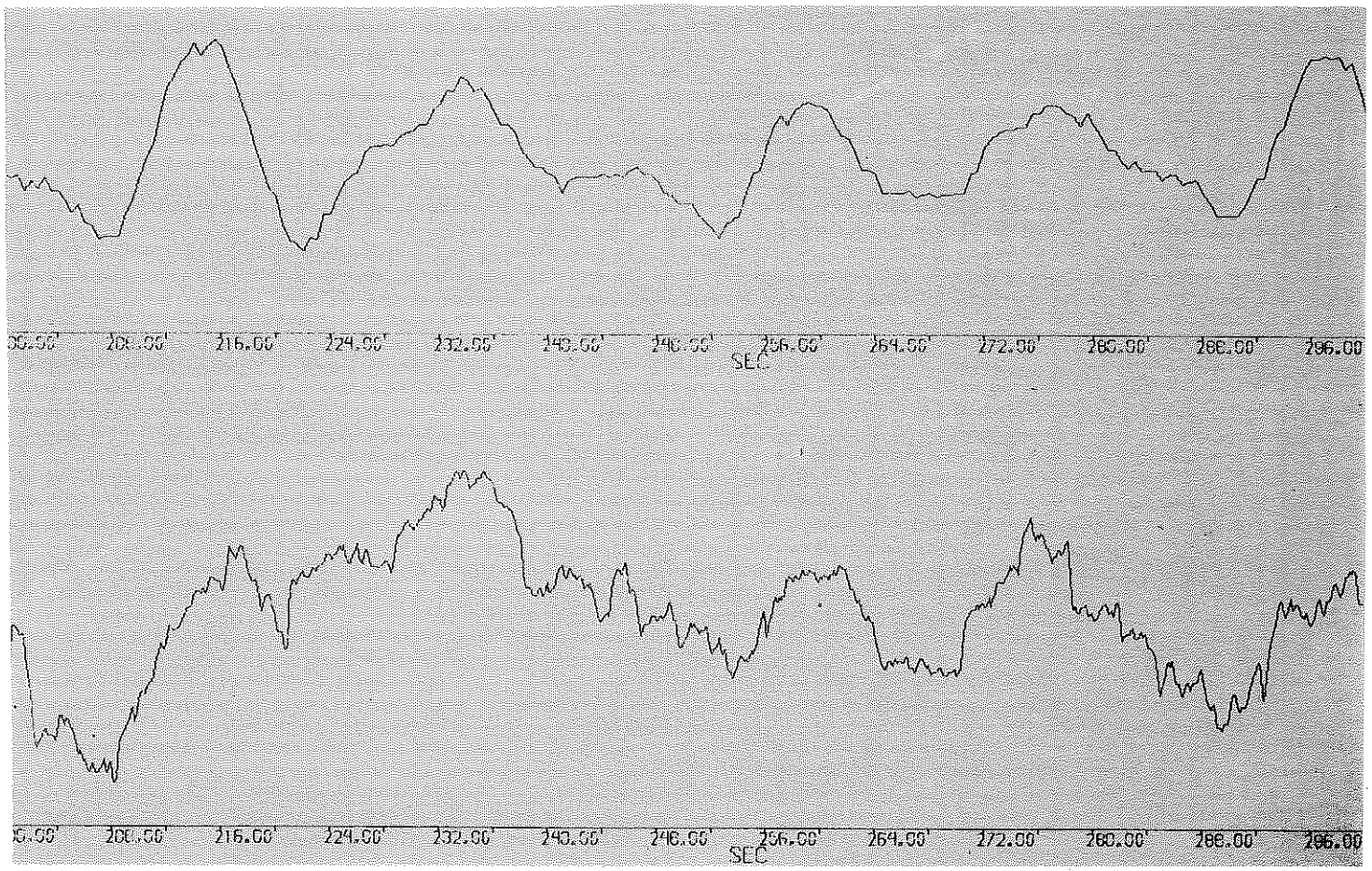

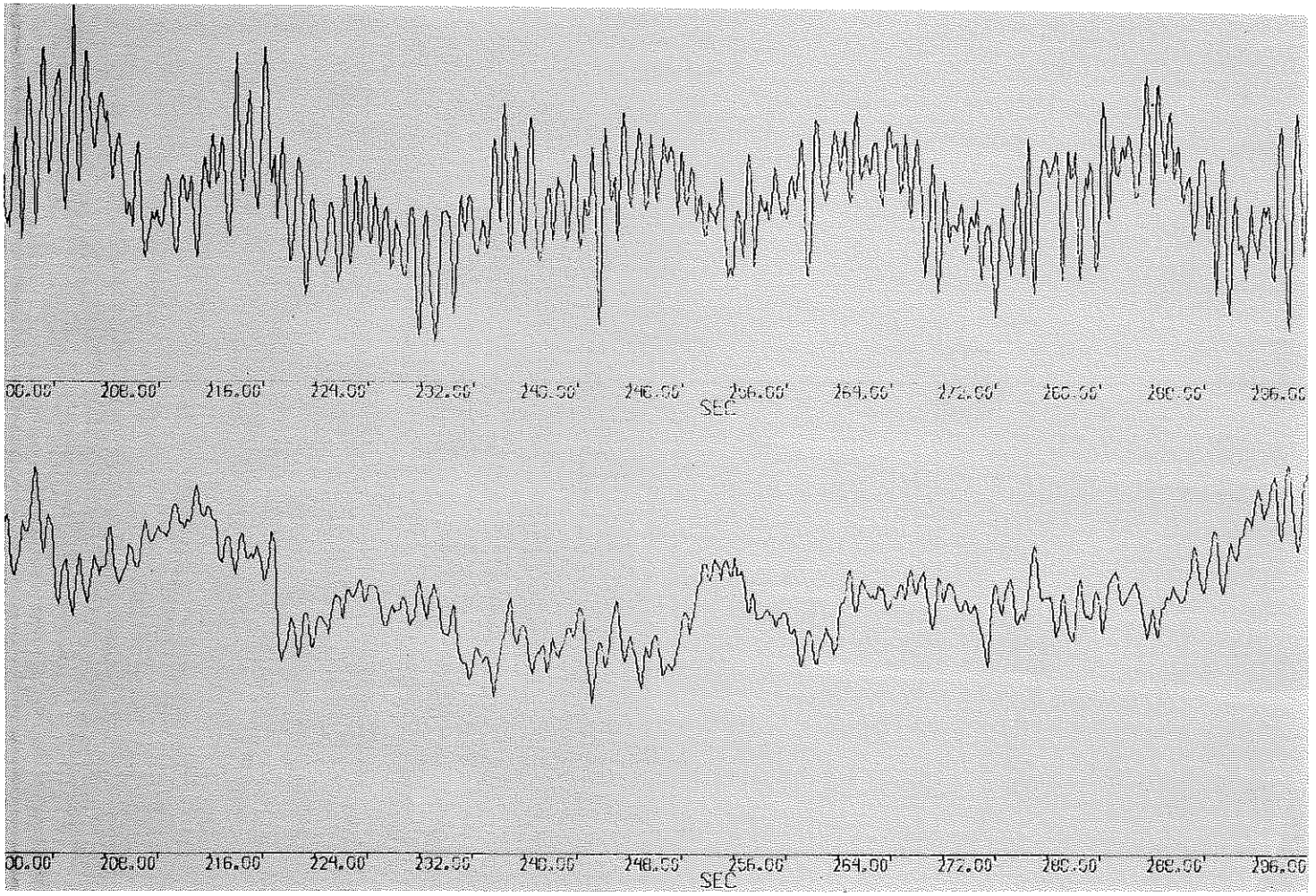

Fig. 3.1. Contd.

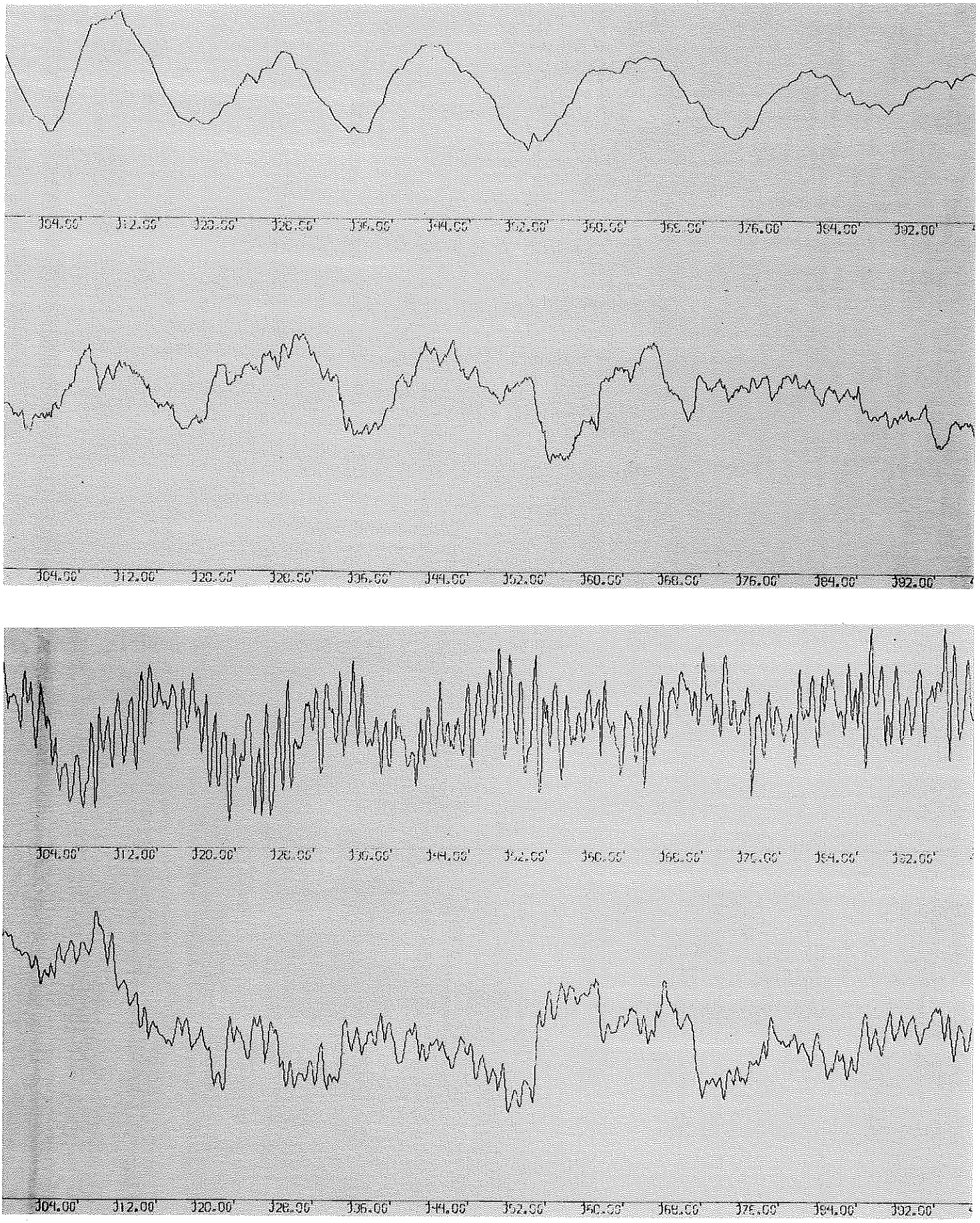

Fig. 3.1. Contd.

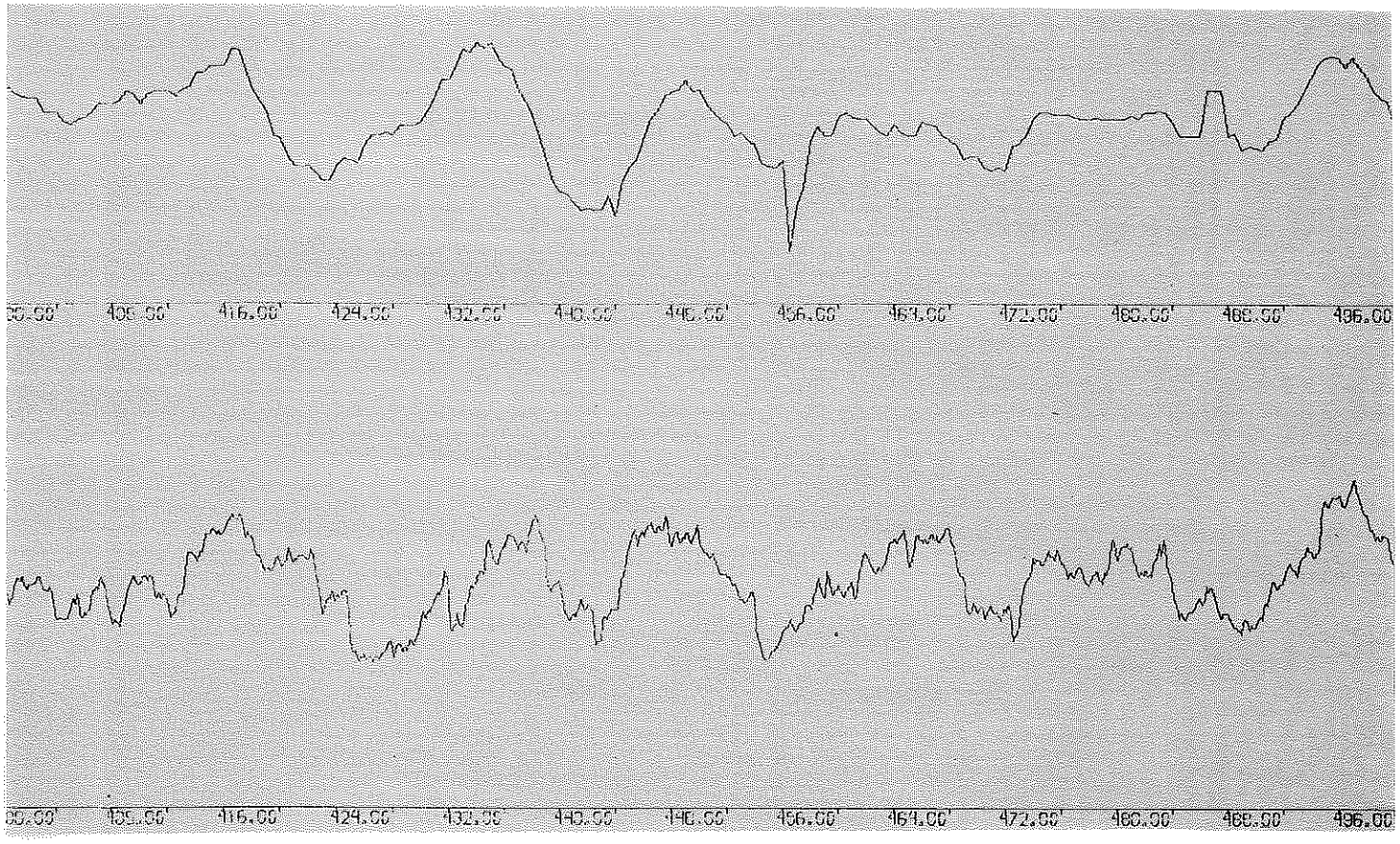
408.00'
416.00'
424.00'
432.00'
440.00'
448.00'
456.00'
464.00'
472.00'
480.00'
488.00'
496.00

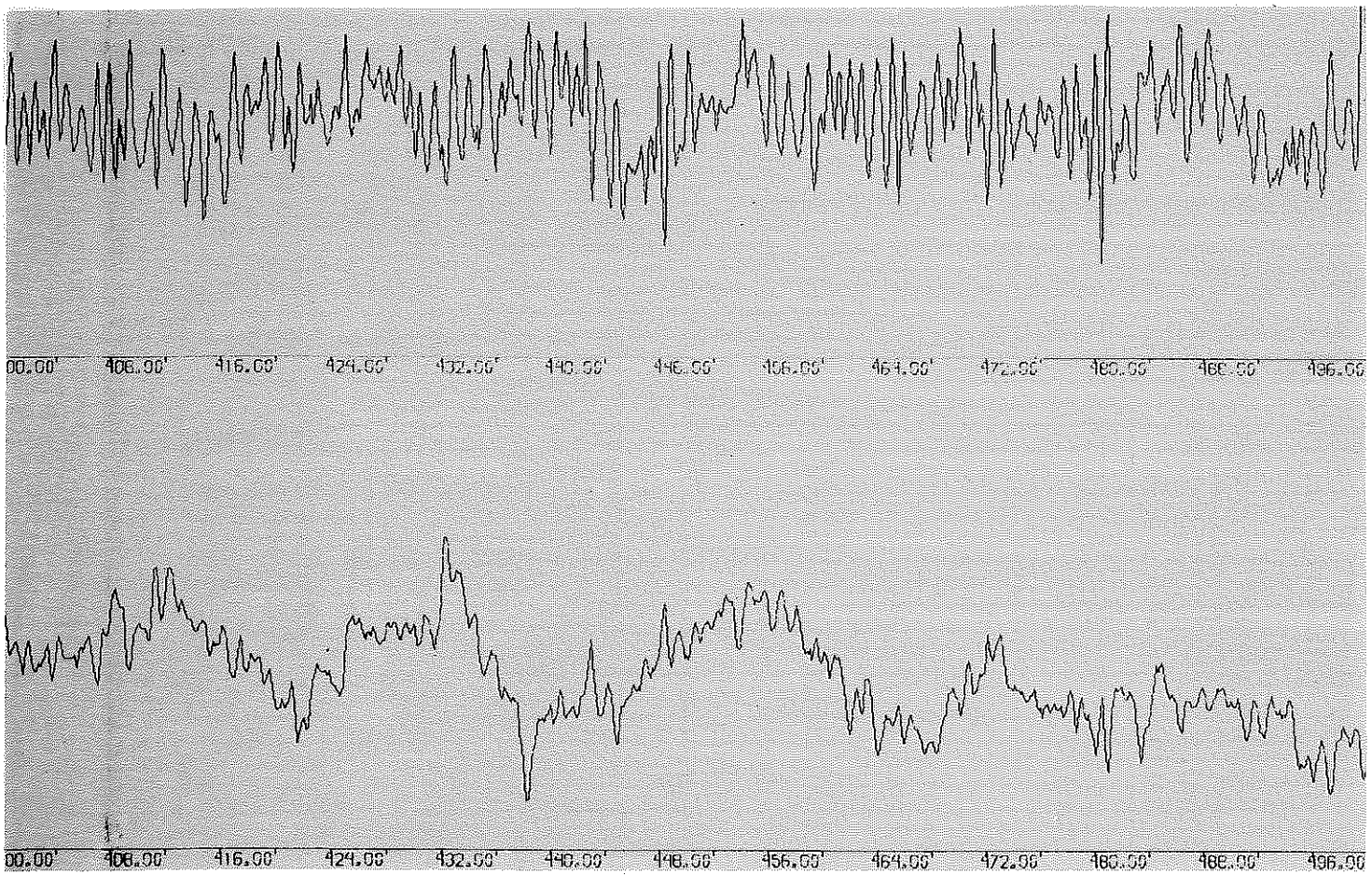
408.00'
416.00'
424.00'
432.00'
440.00'
448.00'
456.00'
464.00'
472.00'
480.00'
488.00'
496.00

Fig. 3.1. Contd.

4. PRELIMINARY ANALYSIS OF DATA

4.1. Introducation

All measurements have been made under normal operating conditions and no artificial disturbances have been applied. Thus all variables arise on equal footing. Furthermore, certain feedback effects from the external power system are to be expected. Hence it is not clear which variables should be considered as inputs and which as outputs. Before proceeding to more elaborate identification methods we will in this section make some preliminary investigations of causality relations between certain pairs of variables.

4.2. Estimation of the impulse response using the fast fourier transform

The cross correlation function between two time series is sometimes used as a source of information about causality relationships. For the present case, as seen from figures 4.1 and 4.2 this is not feasible, since the strong auto-correlations in the time series effectively conceal the information wanted.

Instead, we will estimate the impulse response using a fast fourier transform (FFT) technique. We wish to estimate the coefficients h_r in a relationship

$$y_k = \sum_{-\infty}^{+\infty} h_r u_{k-r} \qquad (4.1)$$

that does not assume a pure causal influence from the time series $\{u_k\}$ to $\{y_k\}$. For a while noise "input" $\{u_k\}$, h_r coincides with the cross correlation function between $\{y_k\}$ and $\{u_k\}$.

The discrete fourier transforms (DFT) of $\{u_k\}$ and $\{y_k\}$ are formed:

$$U_s = \sum_{k=0}^{N-1} u_k \, e^{-2\pi iks/N} \tag{4.2}$$

$$Y_s = \sum_{k=0}^{N-1} y_k e^{-2\pi iks/N}$$

(N = the number of data)

Then the inverse transform of the quotient is formed:

$$\hat{h}_k = \frac{1}{N} \sum_{s=0}^{N-1} \frac{Y_s}{U_s} \, e^{2\pi iks/N} \tag{4.3}$$

Now, $\hat{h}_k$ is an asymptotically unbiased estimate of the aforementioned h_k (4.1). Furthermore, the accuracy of the estimate is reasonable if the signal to noise ratio is not too low and if the response time of the system is not too long, [7]. The transforms are computed using a fast algorithm (FFT), so the computing time to obtain the estimate is very short (1 sec for 1 500 data on a Univac 1108).

4.3. Result of the impulse analysis

The method described in section 4.2 has been applied to several time series pairs, formed from the original data. For each pair two estimates have been calculated, since either of the involved time series can be considered as "input" ($\{u_k\}$ in eq. (4.1)).

Before the analysis the time series were normalized to a variance of 1, so that $h_o = 1$ corresponds to a direct coupling. The result is shown in Fig. 4.3 - 4.7, and each time series pair is commented separately below.

The variable torque is formed as (active current) * (voltage)/ /frequency. Since frequency is sampled only twice a second the new variable also will have this sampling rate. The data records have been made compatible simple by omitting sample points.

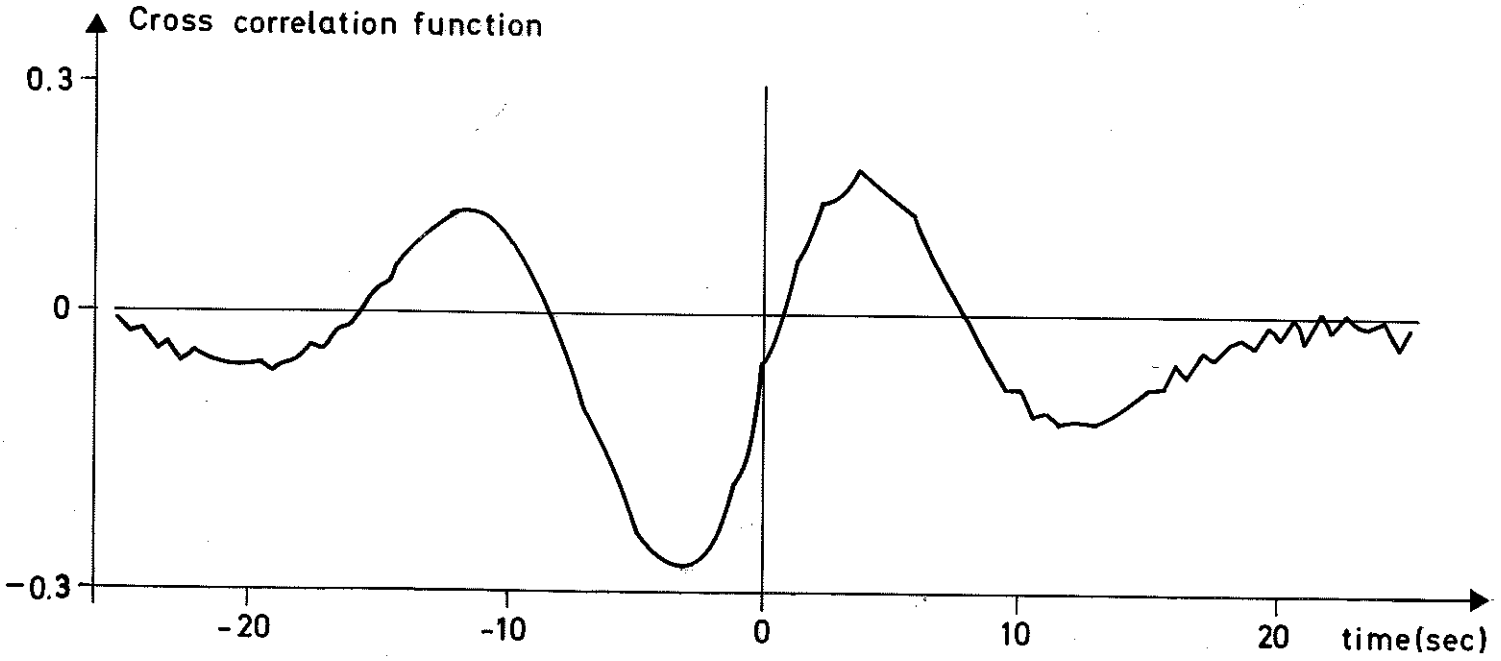

Fig. 4.1. Cross correlation function between frequency and torque. (Positive lag corresponds to frequency leading over torque).

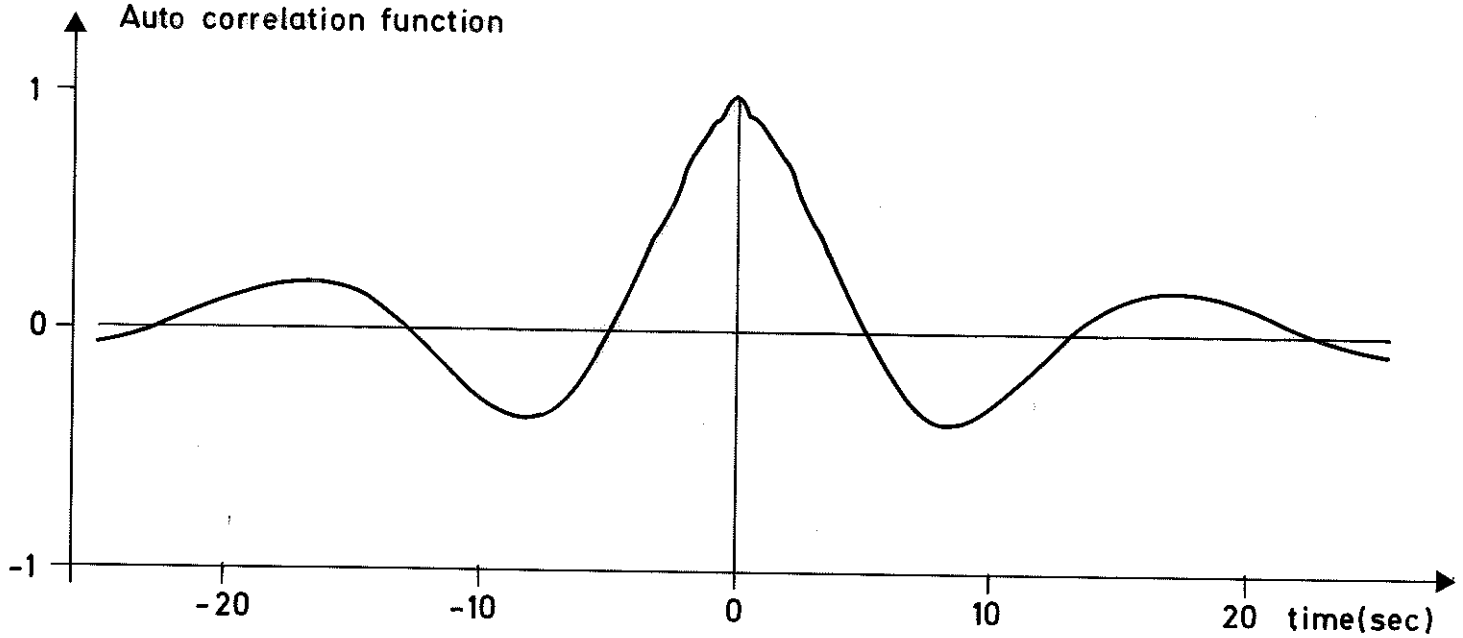

Fig. 4.2. Auto-correlation function for frequency

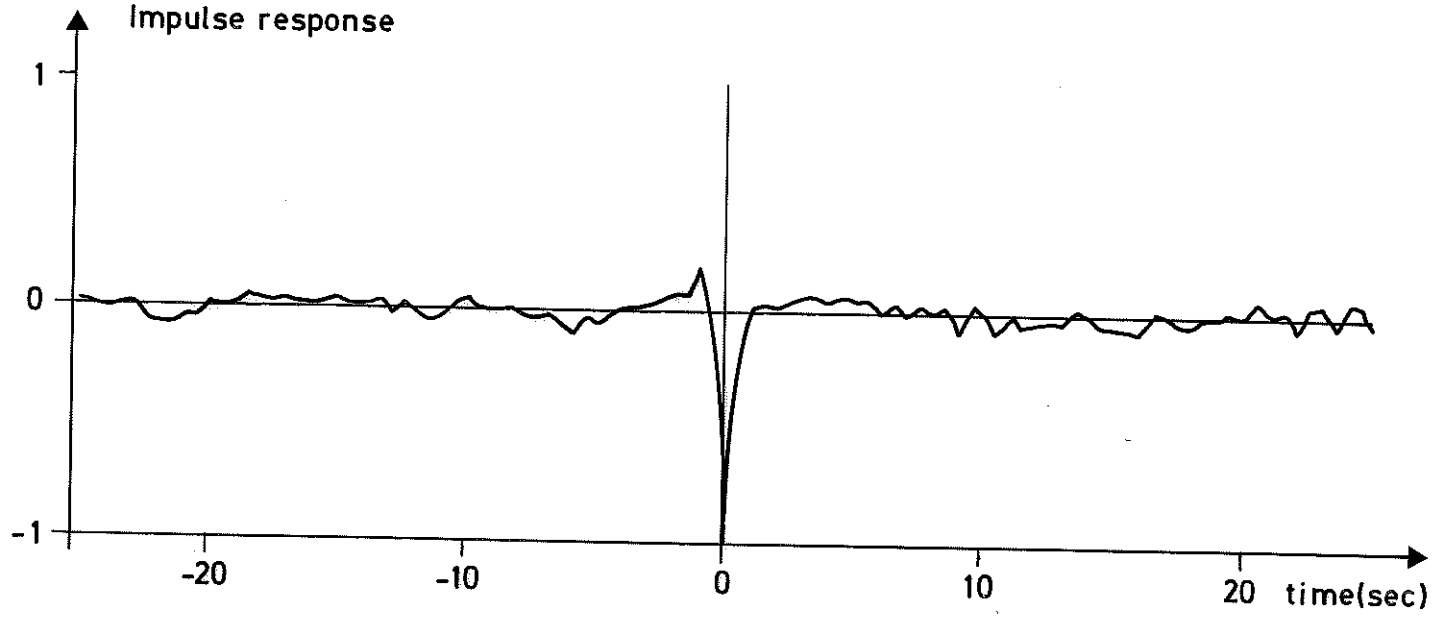

a) Reactive current is input

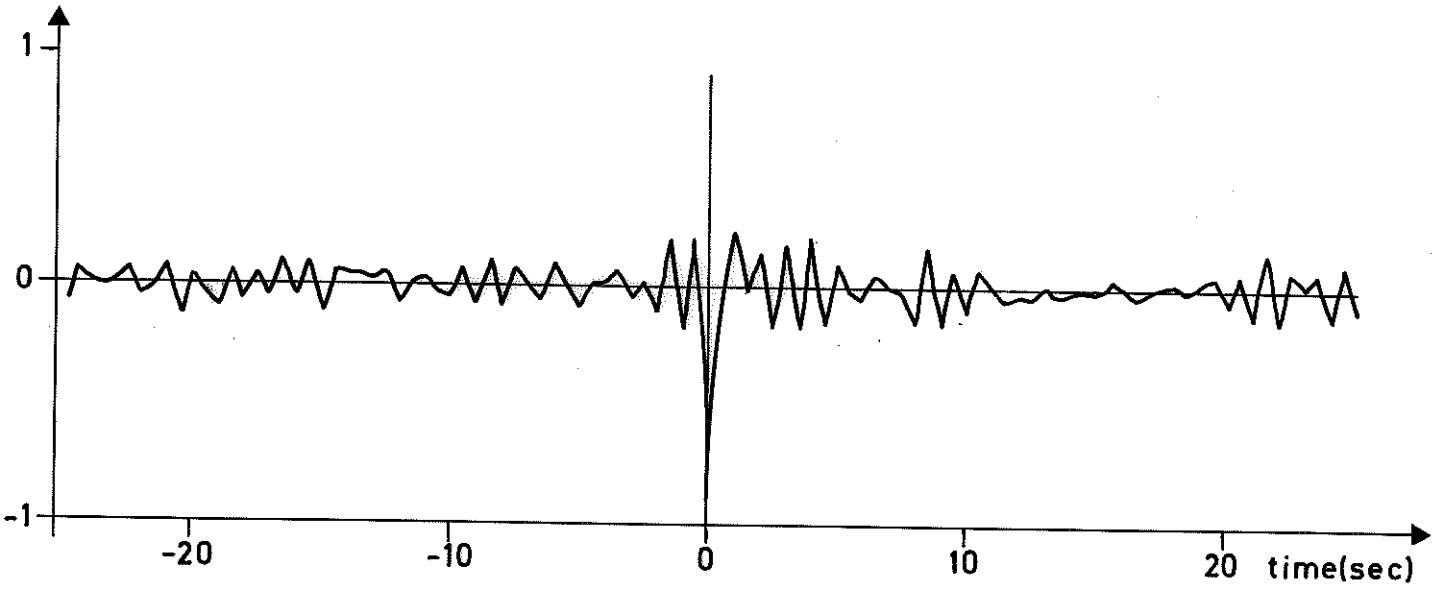

b. Voltage is input

Fig. 4.3. Volatage - Reactive current

The main feature is seen to be a direct term (h_o) relating the two variables. Neglecting the fast responsing modes $p\psi_d$ and $p\psi_q$ this is consistent with eqs (2.19) and (2.20).

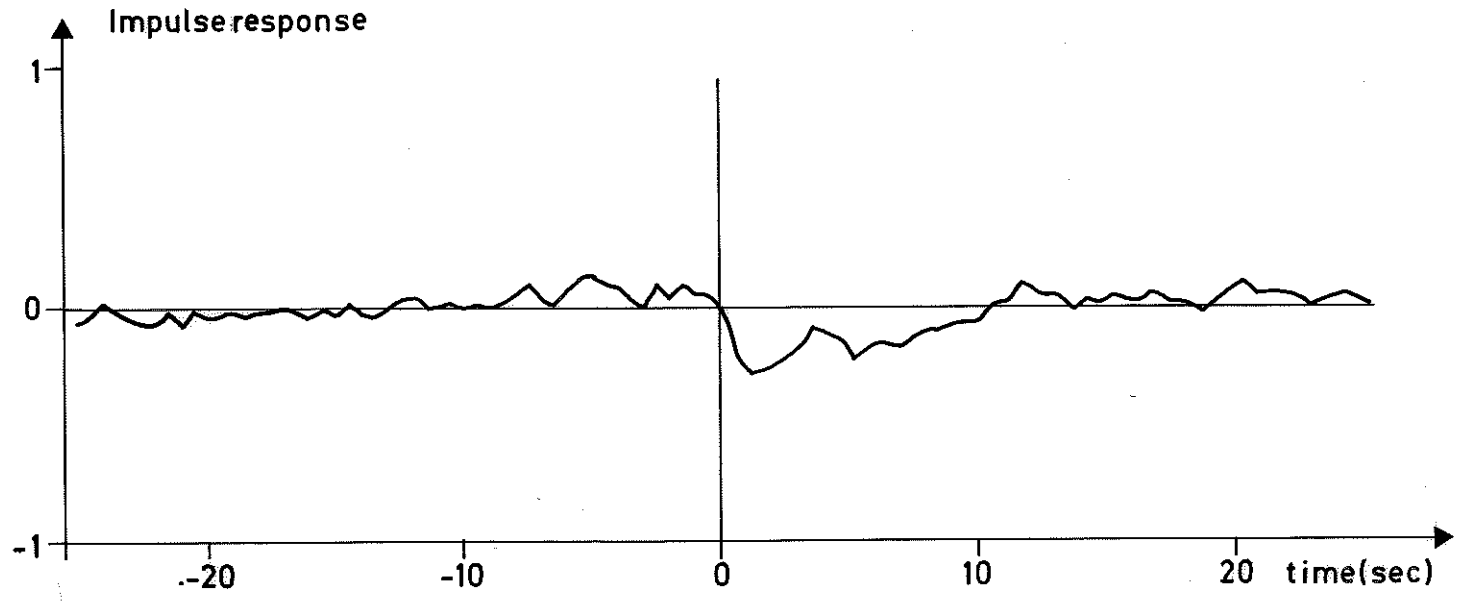

a. Torque is input

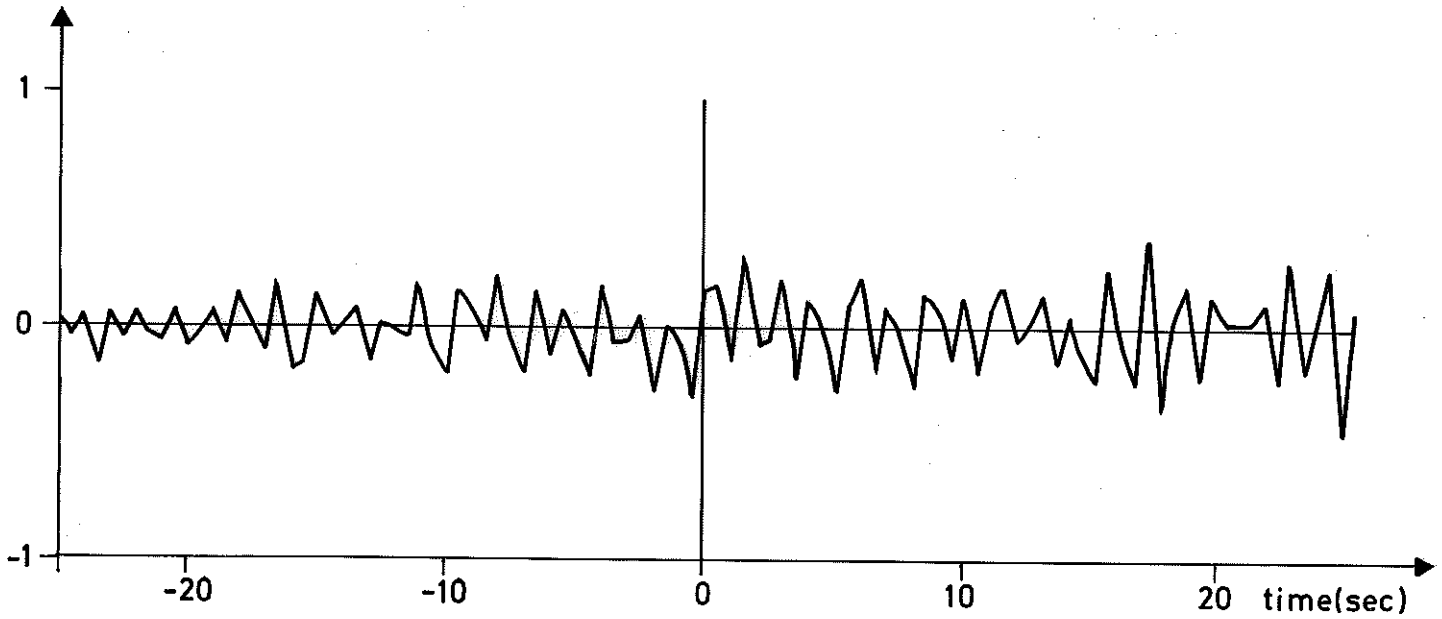

b. Frequency is input.

Fig. 4.4. Frequency - Torque

There is a decisive causality relation from torque to frequency. The response is roughly of $-e^{-at}$ type. In fact it is predicted by eq. (2.32) that the relationship should be a first order system. The disagreement between the actual response and the first order one indicates that assumption (A2.2) in section 2 does not hold strictly.

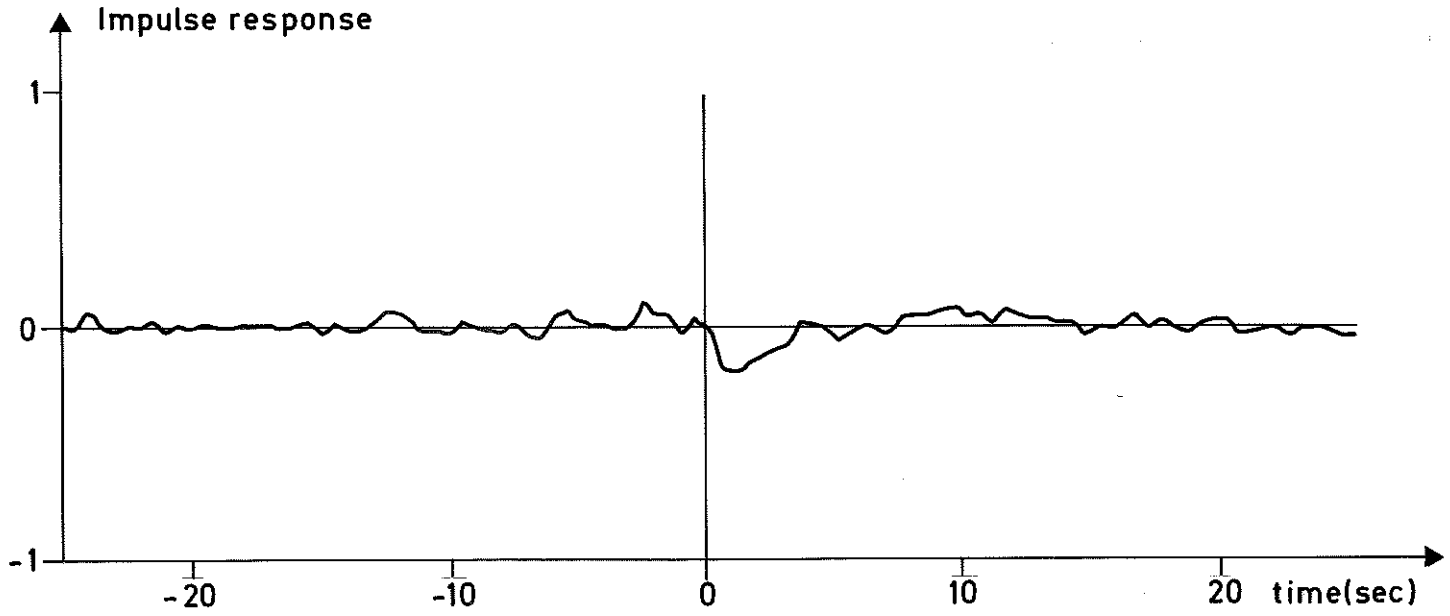

a. Active current is input.

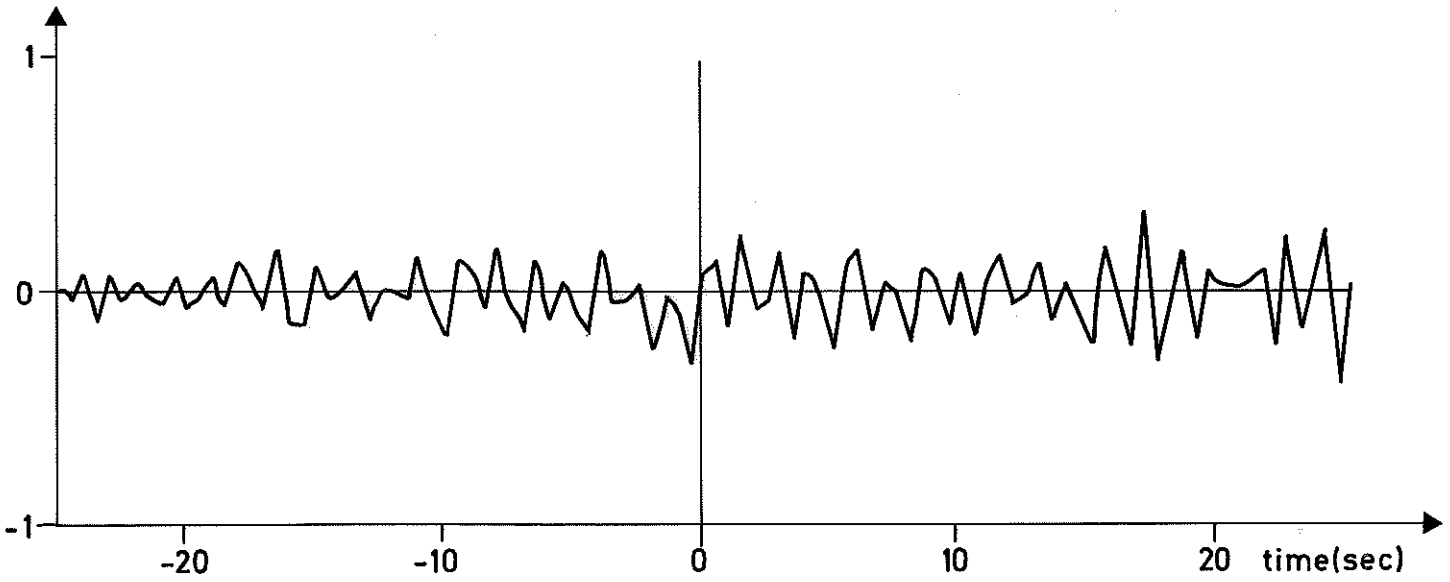

b. Frequency is input

Fig. 4.5. Frequency - Active current

The resemblence with Fig. 4.4 is appearent. As seen from the data plots this is due to the fact that the variations in torque arise from the variations in active current rather than in voltage or frequency

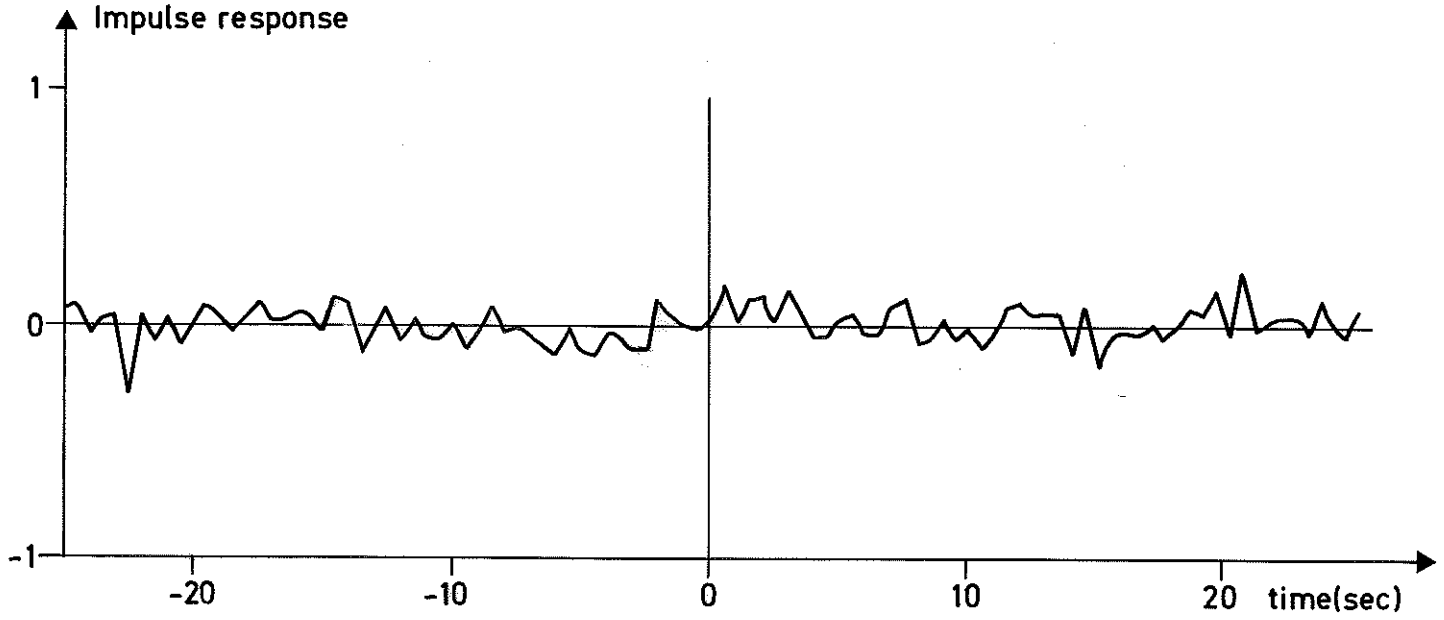

a. Reactive current is input

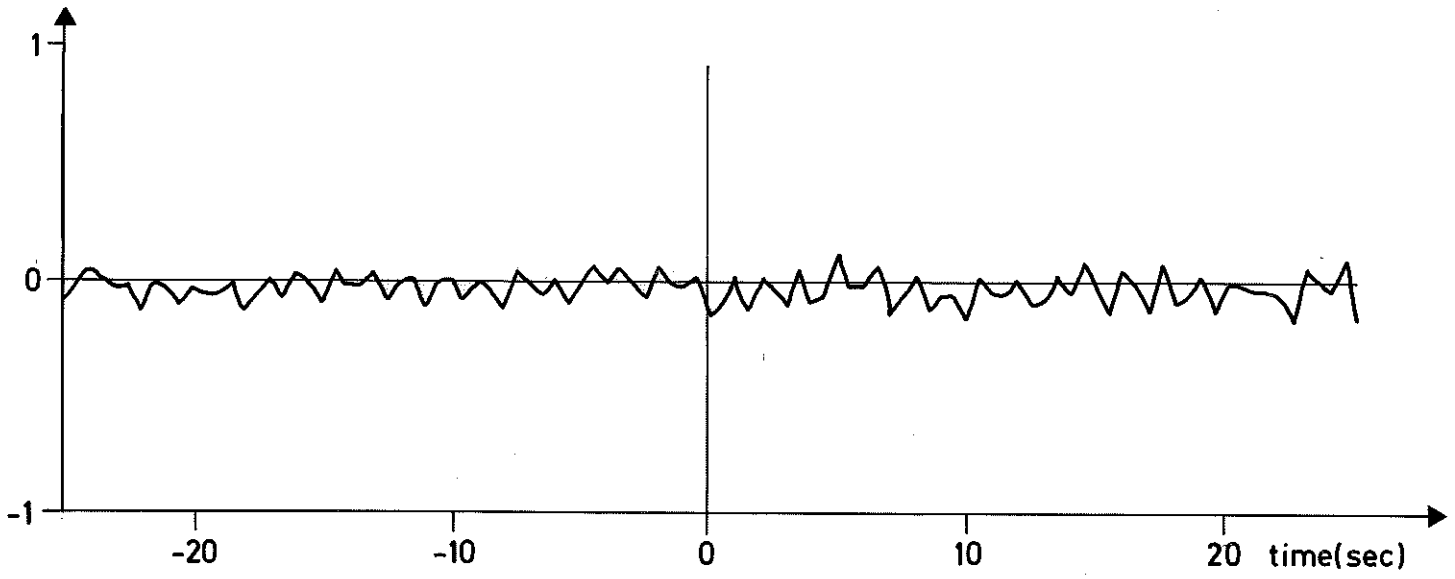

b. Frequency is input

Fig. 4.6. Frequency - Reactive Current

These variables seem to be uncorrelated. Indeed, under assumption (A2.2) they should be independent according to eq (2.29)

4.4. Conclusions

The most decisive input-output pair among those considered is torque to frequency. In the sequel we will concentrate on this pair. It is also inferred that no relationships are purely causual. The variables interact in the machine as well as in the network.

5. SPECTRAL ANALYSIS

5.1. Notations and outline of the method

The cross spectrum, C_{uy}, between input and output signals from a system and the power spectrum of the input, C_{uu}, satisfies the follwing relation

$$C_{uy}(\omega) = H(\omega)C_{uu}(\omega) \tag{5.1}$$

where $H(\omega)$ is the transfer function of the system. See e.g. [8].

The spectral estimates are in principle obtained as fourier transforms of the covariance function estimates. Since the latter estimates have high variances for large lags, they have to be multiplied by a function, a "lag window", that suppresses the values far away from lag zero.

We will here use the so-called Tukey window:

$$W_T(k) = \begin{cases} \frac{1}{2}(1 + \cos(k\pi/M)) & |k| < M \\ 0 & |k| \geq M \end{cases} \tag{5.2}$$

See [8]. The number M is called the width of the lag window.

Thus the spectral estimates $C_{uy}(\omega)$ and $C_{uu}(\omega)$ are obtained as fourier transforms of the product of $W_T(k)$ and the corresponding covariance function estimates.

The terms amplitude and phase spectrum refer to the appropriate quantities of the complex number $C_{uy}(\omega)$. Similarily, the gain and phase estimates are obtained from $H(\omega)$ in (5.1)

By the coherency spectrum is meant the quantity

$$K_{uy}(\omega) = |C_{uy}(\omega)|/(C_{uu}(\omega) \cdot C_{yy}(\omega))^{1/2} \qquad (5.3)$$

It is of crucial importance when to determine confidence intervals for the spectral estimates. In [8], chapter 10.4 formulae for approximate confidence intervals are given:

Gain estimate

$$\hat{G}(\omega) \pm \hat{G}(\omega) \cdot R(\omega)$$

Phase estimate

$$\hat{F}(\omega) \pm \arcsin(R(\omega))$$

where

$$R(\omega) = \sqrt{\frac{2}{\nu-2} f^{(\alpha)}_{2,\nu-2} \left(\frac{1-K^2(\omega)}{K^2(\omega)}\right)} \qquad (5.4)$$

ν is the number of degrees of freedom associated with the lag window, $f^{(\alpha)}_{2,\nu-2}$ is the upper $100(1-\alpha)\%$ point of the $F_{2,\nu-2}$ distribution and $K(\omega)$ is the coherency spectrum.

5.2. Treatment of data before identification

The choice of the lag window parameter M depends on the shape of the true spectrum. A small M will give low variance of the estimate, but will also introduce bias if the true spectrum is not smooth.

The objective of treatment of data, like differencing and prewhitening, is to make the true spectrum smooth so as to allow for smaller M.

In Fig. 5.1 is shown the power spectrum for the frequency time series with M = 100 as well as the estimate when the data has been prewhitened through a tenth order filter and M = 16 used for the filtered data (smooth line).

Since no major difference is obtained it is decided that prewhitening is not necessary.

Another problem is that the currents and voltage is sampled 8 times a second and the frequency twice a second. When the torque is formed as

$$I_r \cdot V/\omega$$

the active effect, $I_r \cdot V$, could be filtered before it is divided by ω. Thereby the information contained in intermediate measurements of I_r and V would be used.

In Fig. 5.2 is shown the power spectrum for active effect.

Very little power is present for frequencies over 1 Hz. Hence it is concluded that no low pass filtering of the active effect signal is needed. Thus the data records are made compatible simply by deleting 3/4 of the active power record. In doing so the power spectrum for the resulting, shorter record is obtained from that in Fig. 5.2 by folding the spectrum at frequency 1 Hz. The distortion of the spectrum from this, is probably less than what low pass filtering with limit 1 Hz would give.

5.3. Results of the identification

The lag parameter M was determined by a "window closing" procedure as described in [8]. A suitable value was found to be 40. Once the pre-treatment of data and the lag parameter are determined the calculation of spectra is straightforward.

The result of the identification is given in Fig. 5.3 and 5.4 as a Bode plot of the transfer function from torque (in p.u.) to frequency (in rad/sec).

To get some information about the reliability of the estimate we may compute approximate confidence intervals.

Since these do not include bias effects we choose a larger value of M(M=100) for the confidence analysis. As mentioned in section 5.2 a larger value will give smaller bias but larger variance for the estimate.

In Fig. 5.5 and 5.6 95 % confidence intervals have been marked out for the estimates with lag parameter M=100. Estimates for which $R(\omega)$ (defined in (5.4)) is greater than 1 have been omitted and replaced by interpolated values.

($R(\omega) > 1$ corresponds to $K^2(\omega) < 0.18$ with $\nu = 32$ and $f_{2,30}^{(0.05)} = 3.32$)

5.4. Conclusions

Fig. 5.3 and 5.4 appearently preclude a first order system for the torque to frequency relationship. This is consistent with the indicated disagreement with a first order system impulse response obtained in Fig. 4.4. However, taking into account the confidence intervals in Fig. 5.5 and 5.6 it is seen that statements on system order cannot be made with a great degree of significance. The tendency towards -180° for the phase estimate should not be taken as an evidence of higher order system. Phase estimates may be quite irrelevant for frequencies over a tenth of the Nyquist frequency. For example, any phase estimate for a first order system tends to -180° if the input signal is piecewise constant.

Consequently we conclude that the spectral analysis indicates that the transfer function from torque to frequency is of degree greater than one. However, this is merely an indication, and has no great degree of significance.

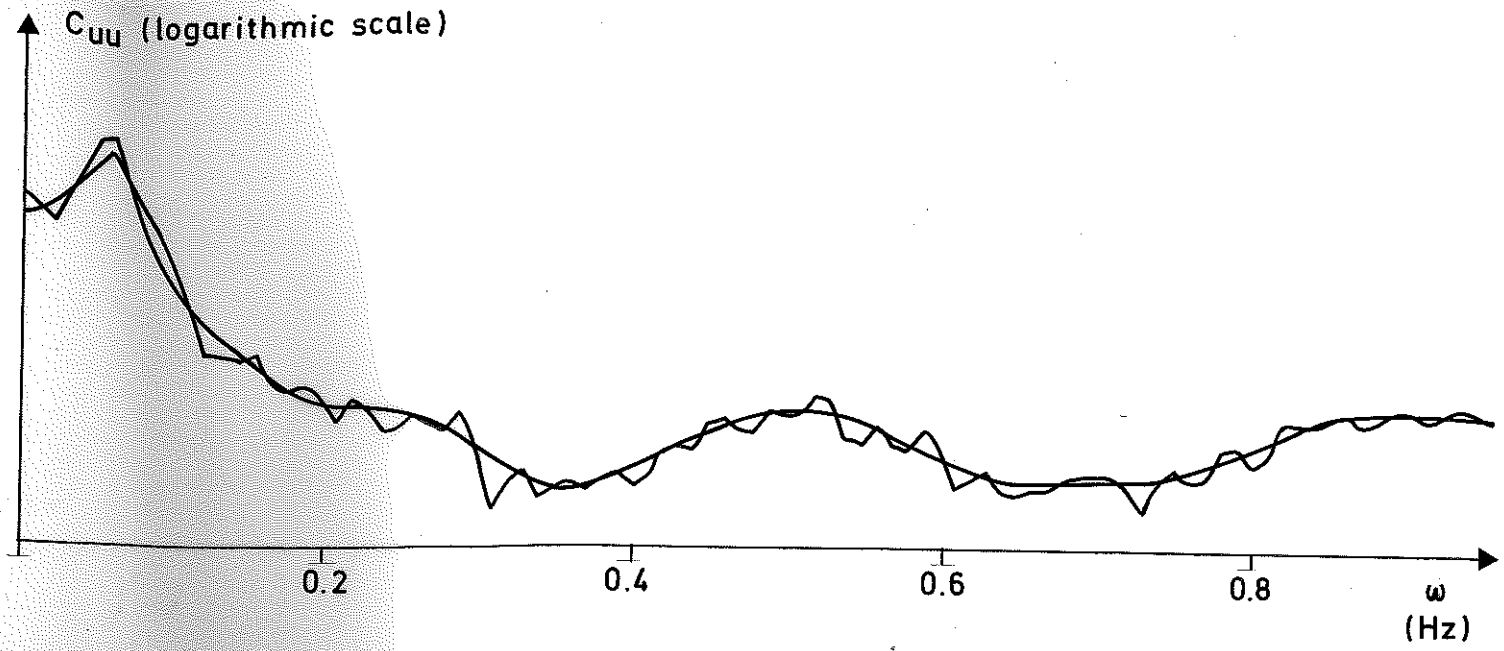

Fig. 5.1. Power spectrum for frequency. Rough line: The lag parameter M = 100. Smooth line: The time series has been prewhitened through a tenth order filter and M=16 has been used on the filtered data. The spectrum is obtained partly from the filter parameters and partly from the spectrum of the filtered data.

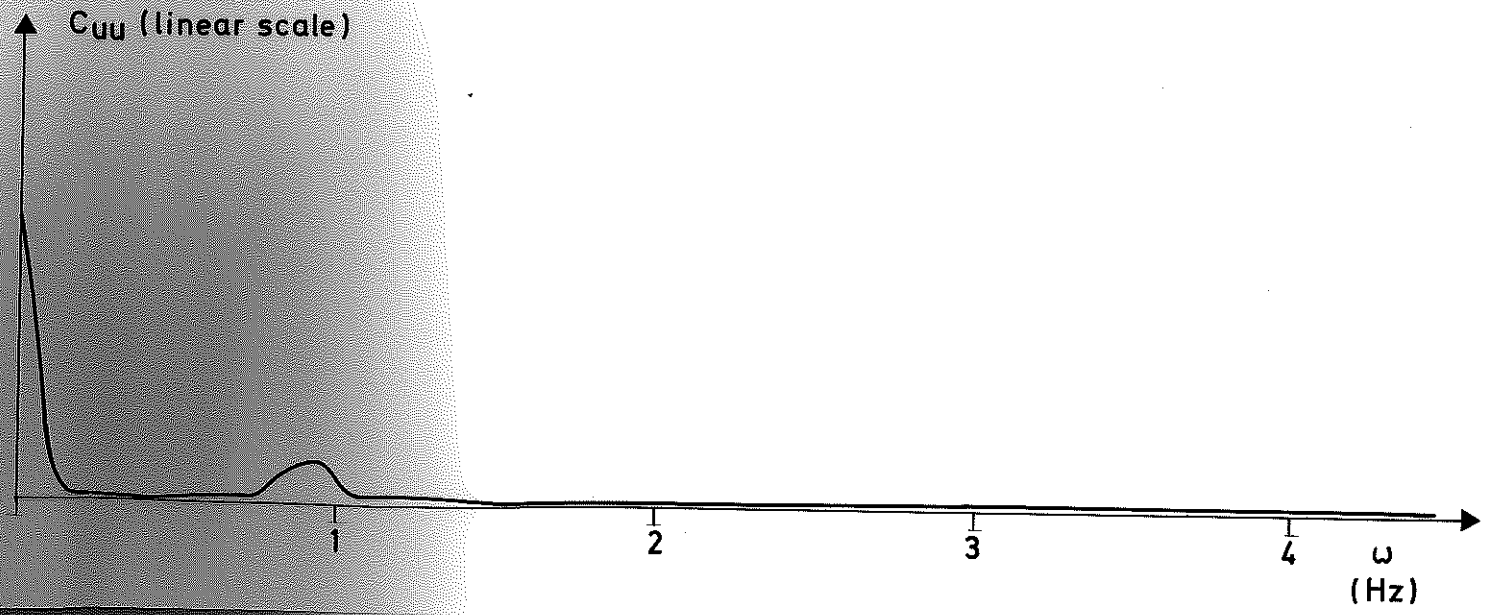

Fig. 5.2. Power spectrum for active effect. Note: Linear scale on y-axis!

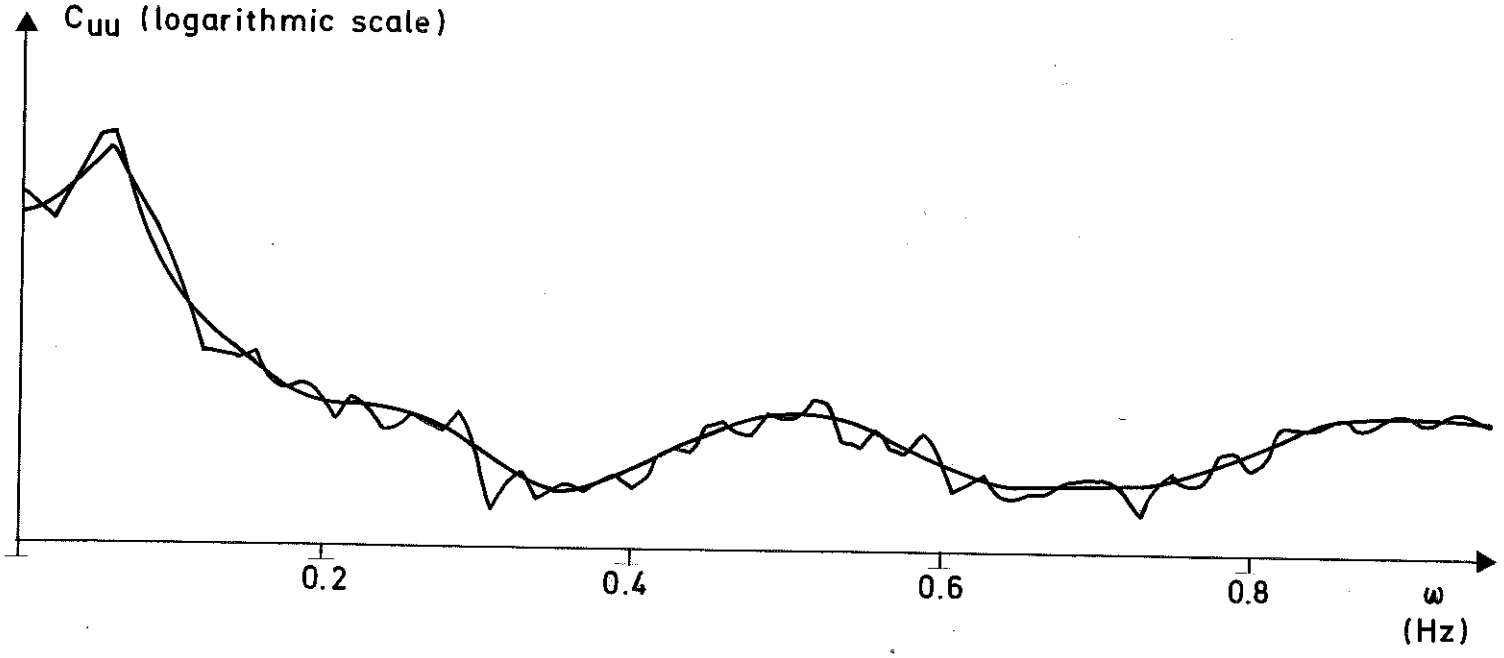

Fig. 5.1. Power spectrum for frequency. Rough line: The lag parameter M = 100. Smooth line: The time series has been prewhitened through a tenth order filter and M=16 has been used on the filtered data. The spectrum is obtained partly from the filter parameters and partly from the spectrum of the filtered data.

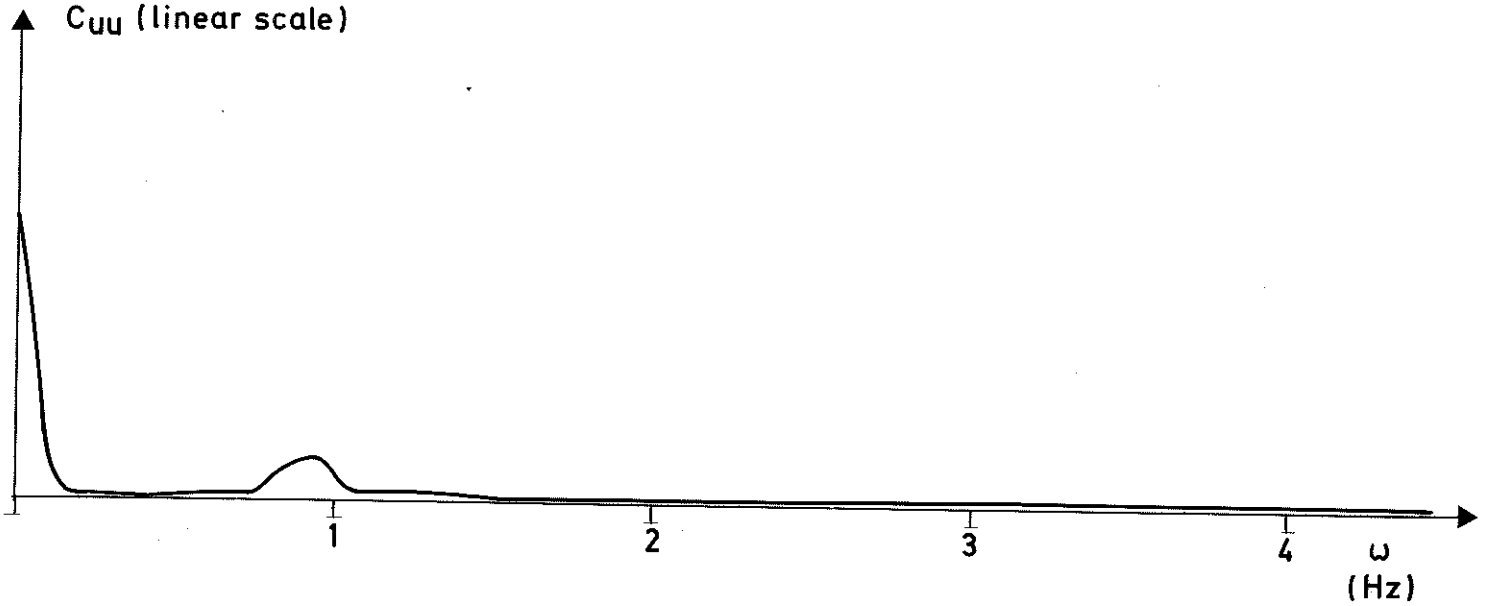

Fig. 5.2. Power spectrum for active effect. Note: Linear scale on y-axis!

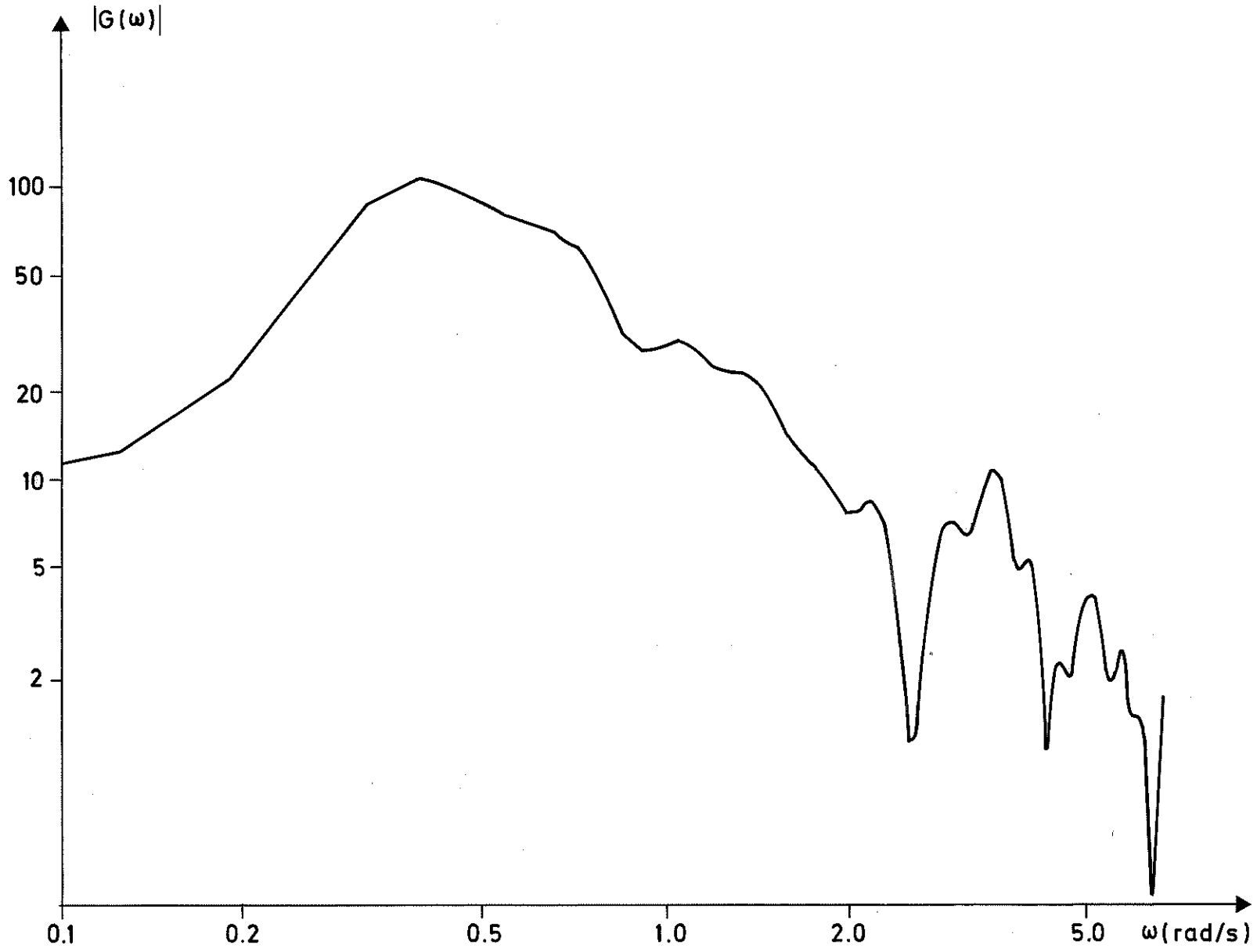

Fig. 5.3. Amplitude Bode plot of estimated transfer function from torque (in p.u.) to frequency (in rad/s)

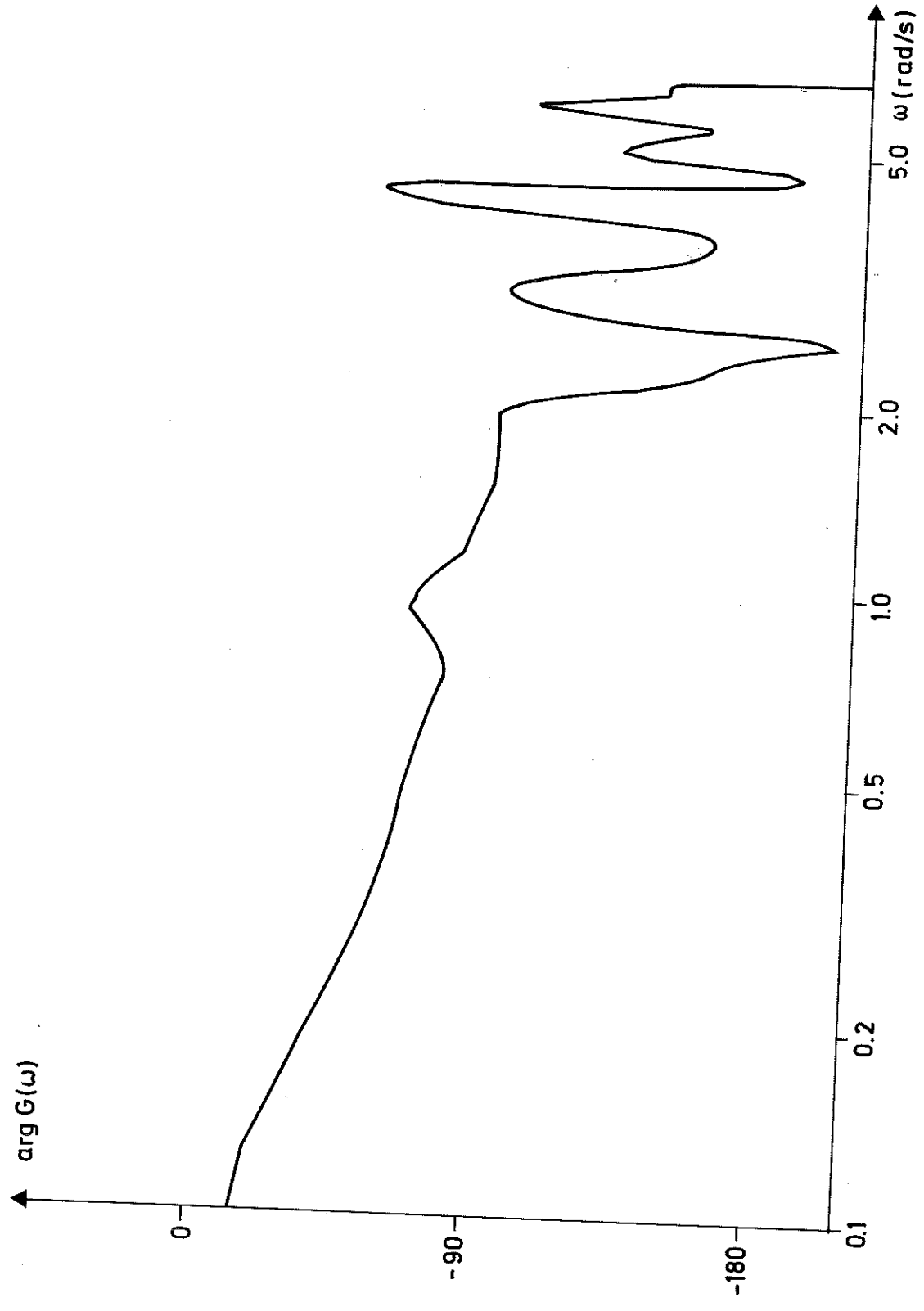

Fig. 5.4. Phase Bode plot of estimated transfer function from torque to frequency.

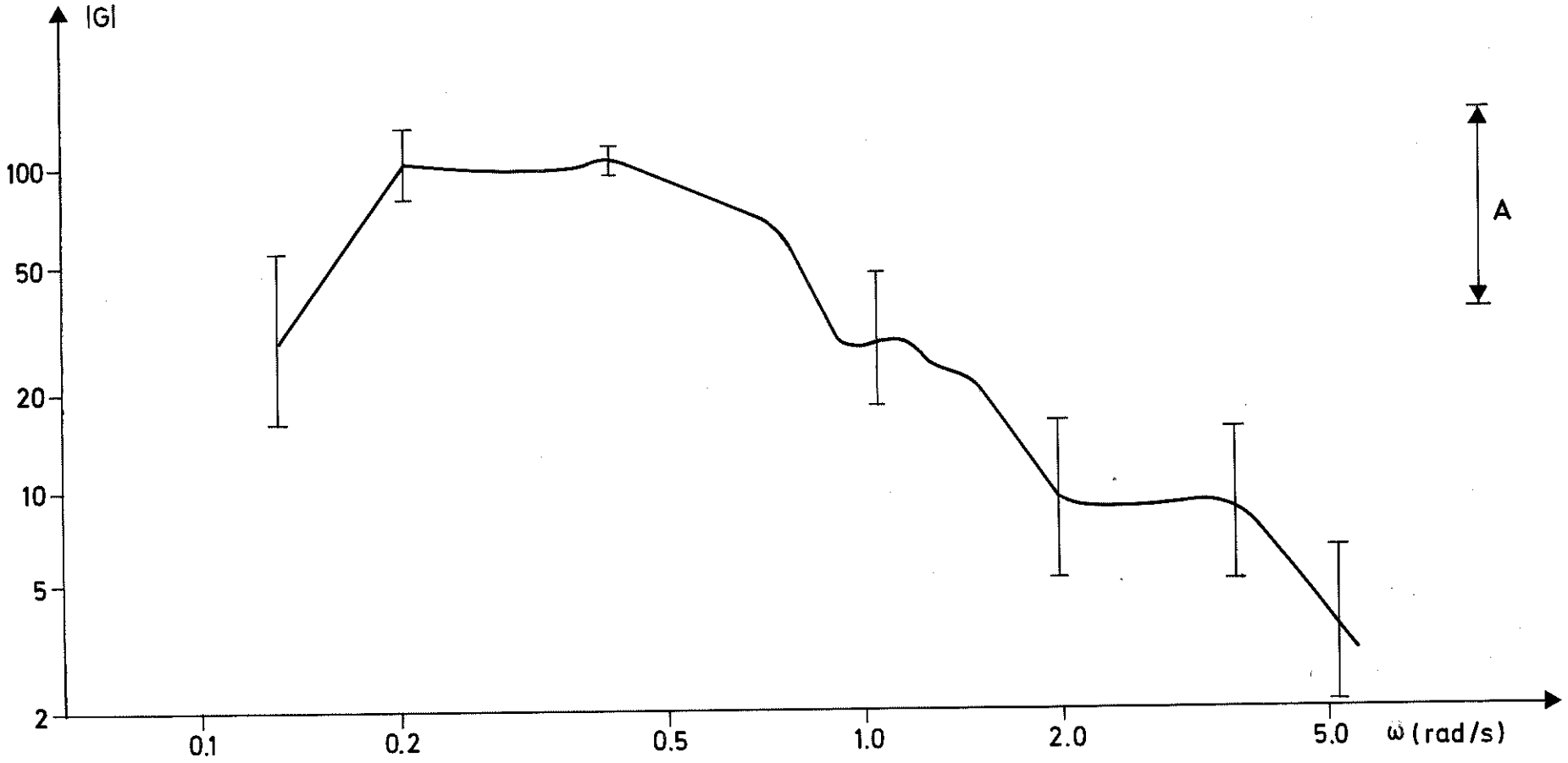

Fig. 5.5. Amplitude Bode plot of estimated transfer function from torque (in p.u.) to frequency (in rad/s). A lag parameter M=100 has been used. 95% confidence intervals are marked out.Estimates,whose confidence interval is larger than distance A have been omitted and replaced by interpolated values.

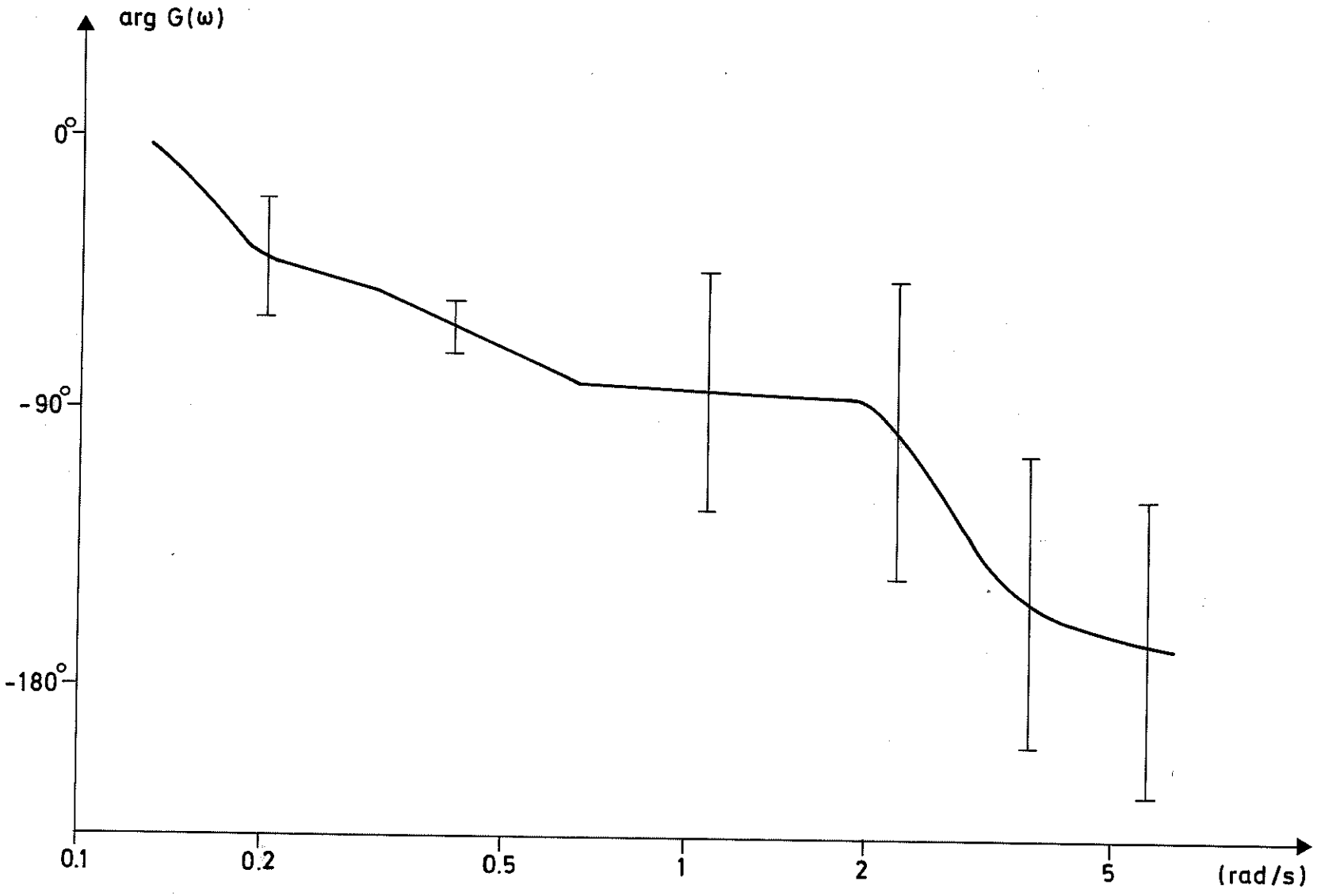

Fig. 5.6. Phase Bode plot of estimated transfer function from torque to frequency. A lag parameter M=100 has been used.95% confidence intervals are marked out.Estimates,whose confidence interval is larger than 180° have been omitted and replaced by interpolated values.

6. ESTIMATION OF PARAMETERS IN A FIRST ORDER STATE SPACE MODEL

In this section we try to determine D and J in the transfer function $G_{M\omega}(s)$, derived in section 2.

$$G_{M\omega}(s) = \frac{1/D}{1+sJ/D} \tag{2.32}$$

The general formulation of this problem is: Estimate the parameter vector, α, in a model of a process from which we have input/output samples. It is assumed that the continuous-time deterministic model can be described by

$$\frac{dx(t)}{dt} = A(\alpha)x(t) + B(\alpha)u(t) \tag{6.1}$$

$$y(t) = C(\alpha)x(t) + D(\alpha)u(t) \tag{6.2}$$

$$x(t_o) = x_o(\alpha) \tag{6.3}$$

where x is the n_x-dimensional state vector, u is n_u-dimensional input vector, y is the n_y-dimensional output vector and α the n_α-dimensional parameter vector. A, B, C and D are $n_x \times n_x$, $n_x \times n_u$, $n_y \times n_x$ and $n_y \times n_u$ matrices respectively.

In this section we describe the data preparation and present the result of the identification, but first we present a short summary of the identification method.

6.1. Outline of the Identification method

We assume that the discrete-time stochastic version of (6.1) to (6.3) can be written

$$x(k+1) = \Phi(\alpha)x(k) + \Gamma(\alpha)u(k) \tag{6.4}$$

$$y(k) = \Theta(\alpha)x(k) + D(\alpha)u(k) + e(k) \tag{6.5}$$

$$x(1) = x_o(\alpha)$$

where

$\{x(k),\ k=1,2,\ldots,N\}$ is the state-sequence

$\{u(k),\ k=1,2,\ldots,N\}$ is the input-sequence

$\{y(k),\ k=1,2,\ldots,N\}$ is the output sequence

and

$\{e(k),\ k=1,2,\ldots,N\}$ is a sequence of independent equally distributed gaussian variables with zero mean and covariance R.

For the structure (6.4) to (6.6) the likelihood function is given [9] by

$$-\log L(\alpha,R) = \frac{N}{2}\log(\det R) + \frac{1}{2}\sum_{k=1}^{N} \varepsilon^T(k)R^{-1}\varepsilon(k)$$

$$+ \frac{Nn_y}{2}\log 2\pi \tag{6.7}$$

The maximization of $L(\alpha,R)$ can be performed separately with respect to α and R. It was shown in [10] that the maximum of $L(\alpha,R)$ is obtained by finding α, which minimizes

$$V(\alpha) = \det \sum_{k=1}^{N} \varepsilon(k)\varepsilon(k)^T \tag{6.8}$$

The maximization with respect to R can then be done analytically to yield

$$\hat{R} = \frac{1}{N} \sum_{k=1}^{N} \varepsilon(k)\varepsilon^T(k) \tag{6.9}$$

6.2. Data Preparation

As the original data have different sampling-rates and the air-gap torque was not measured directly we had to prepare data to fit into available identification programs.

First we used linear interpolation to obtain the three missing ω-values between the measured values. From the interpolated ω-sequence and the I_r and V-sequences we formed three new sequences, which were used in the identification programs:

1) $\{\delta\omega(k),\ k=1,2,\ldots,N\}$

2) $\{\delta M(k),\ k=1,2,\ldots,N\}$

3) $\{\Delta M(k),\ k=1,2,\ldots,N\}$

The residuals $\varepsilon(k)$ are defined by

$$\varepsilon(k) = \hat{y}(k) - y(k)$$

where $\hat{y}(k)$ is the output of the model using the current value of the parameter vector $(\hat{\alpha})$.

where

$$\delta\omega(k) = \omega(k) - \frac{1}{N}\sum_{i=1}^{N}\omega(i)$$

$$\delta M(k) = \omega_o\left[V(k)I_r(k)/\omega(k) - \frac{1}{N}\sum_{i=1}^{N}V(i)I_r(i)/\omega(i)\right]$$

$$\Delta M(k) = \omega_o\left[V(k+1)I_r(k+1)/\omega(k+1) - V(k)I_r(k)/\omega(k)\right]/T$$

In these formulas $V(k)$ and $I_r(k)$ are expressed in p.u., $\omega(k)$ and ω_o in rad/s. The number of samples used in the identification is denoted by N, (N=1000 with rare exceptions).

The three sequences were grouped into two series:

A) δM - $\delta\omega$ -series

B) ΔM- $\delta\omega$ -series

6.3. Result of the Identification, δM-$\delta\omega$-series

The model relating electrical torque to angular frequency was derived in section 2, eq. (2.30)

$$\frac{d(\delta\omega)}{dt} = -\frac{D}{J}\,\delta\omega - \frac{1}{J}\,\delta M \qquad (6.10)$$

The estimated parameter values are:

$D = 0.0766$ p.u./(rad/s)

$J = 0.173$ p.u./(rad/s^2)

The transfer function $G_{M\ddot{\omega}}(s)$ then becomes:

$$G_{M\omega}(s) = \frac{13.0}{1+s2.26} \qquad (6.11)$$

where M is expressed in p.u. and ω in rad/s. The results reported by Dr. Stanton [4] are

$$G_{P\dot{\omega}}(s) = G_{r\omega}(s)/V_o = \frac{12.5/1.04}{1+s2.5}$$

The combined rotor inertia quoted by the manufactuer is:

$J = 0.022$ p.u./(rad/s^2)

In Fig. 6.1 we show

a) the input, δM

b) the output, $\delta\omega$

c) the output from the deterministic model, $\delta\omega_d$

d) the error of the deterministic model, $e_d = \delta\omega - \delta\omega_d$

The estimated value of J differs from the value quoted by the manufacturer by a factor 8. The model (6.10) can only explain a minor part of the output. A possible explanation is that we have assumed that δM is constant over the sampling interval, but in Fig. 6.1 we observe the rapid variations in δM.

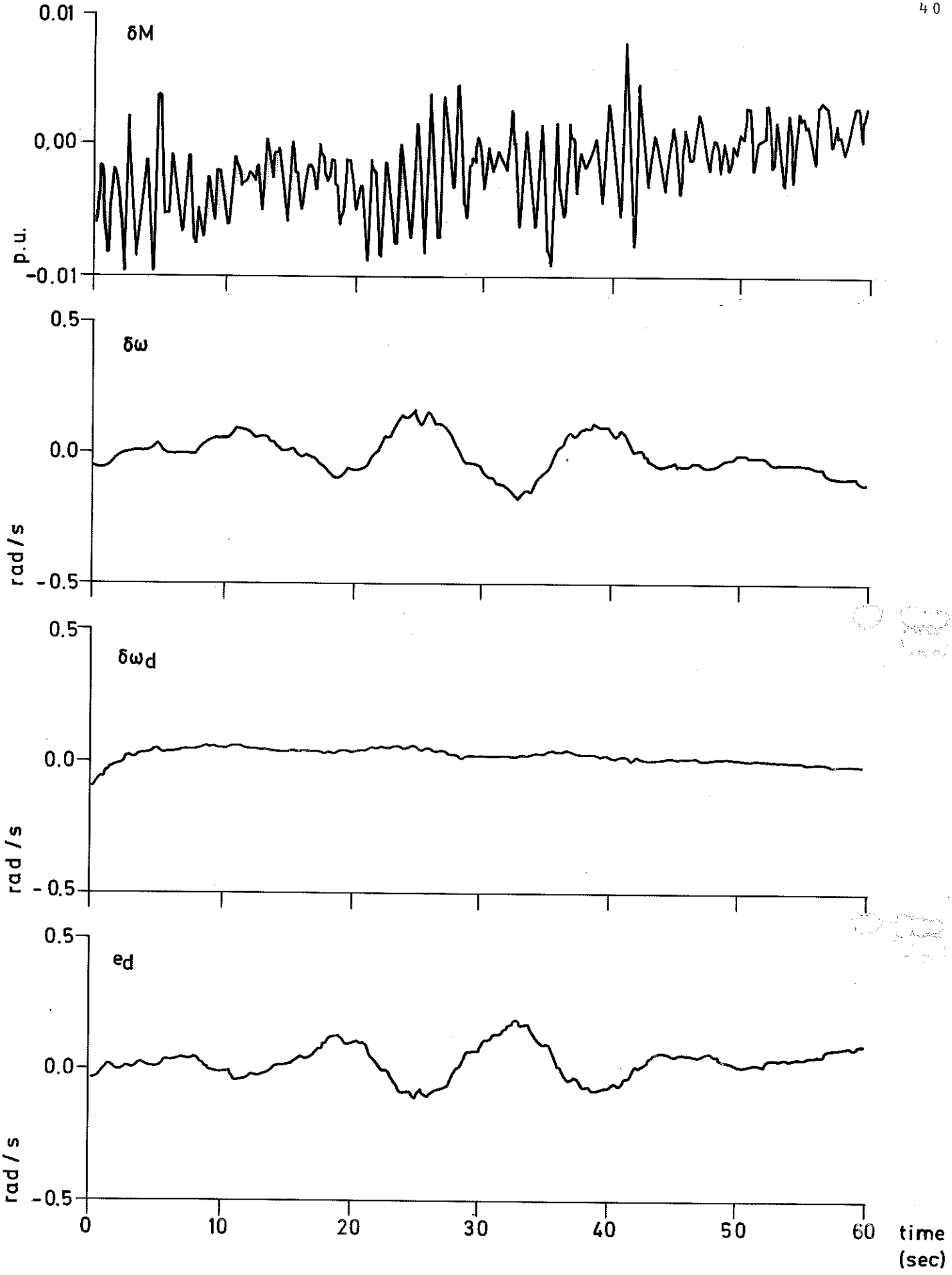

Fig. 6.1. Time-response for the first order state space model (6.10).

6.4. Result of the identification, ΔM-$\delta\omega$-series

In order to investigate the validity of the assumption that $\delta M(t)$ is constant over the sampling interval, we used $\Delta M(t)$ as input to a second order model

$$\frac{d(\delta\omega)}{dt} = -\frac{D}{J}\,\delta\omega - \frac{1}{J}\,\delta M \qquad (6.12)$$

$$\frac{d(\delta M)}{dt} = \Delta M \qquad (6.13)$$

assuming that $\delta M(t)$ varies lineary between the measured values.

In this case the estimated parameter values are:

$D = 0.0965$ p.u./(rad/s)

$J = 0.161$ p.u./(rad/s^2)

In Fig. 6.2 we show:

a) the input, ΔM
b) the output, $\delta\omega$
c) the output from the deterministic model, $\delta\omega_d$
d) the error of the deterministic model, $e_d = \delta\omega - \delta\omega_d$

The values of the parameters are changed significantly. This indicates that the assumption, that $\delta M(t)$ is constant

over the sampling interval is too crude. Still the first order model (6.12) can only explain a minor part of the output.

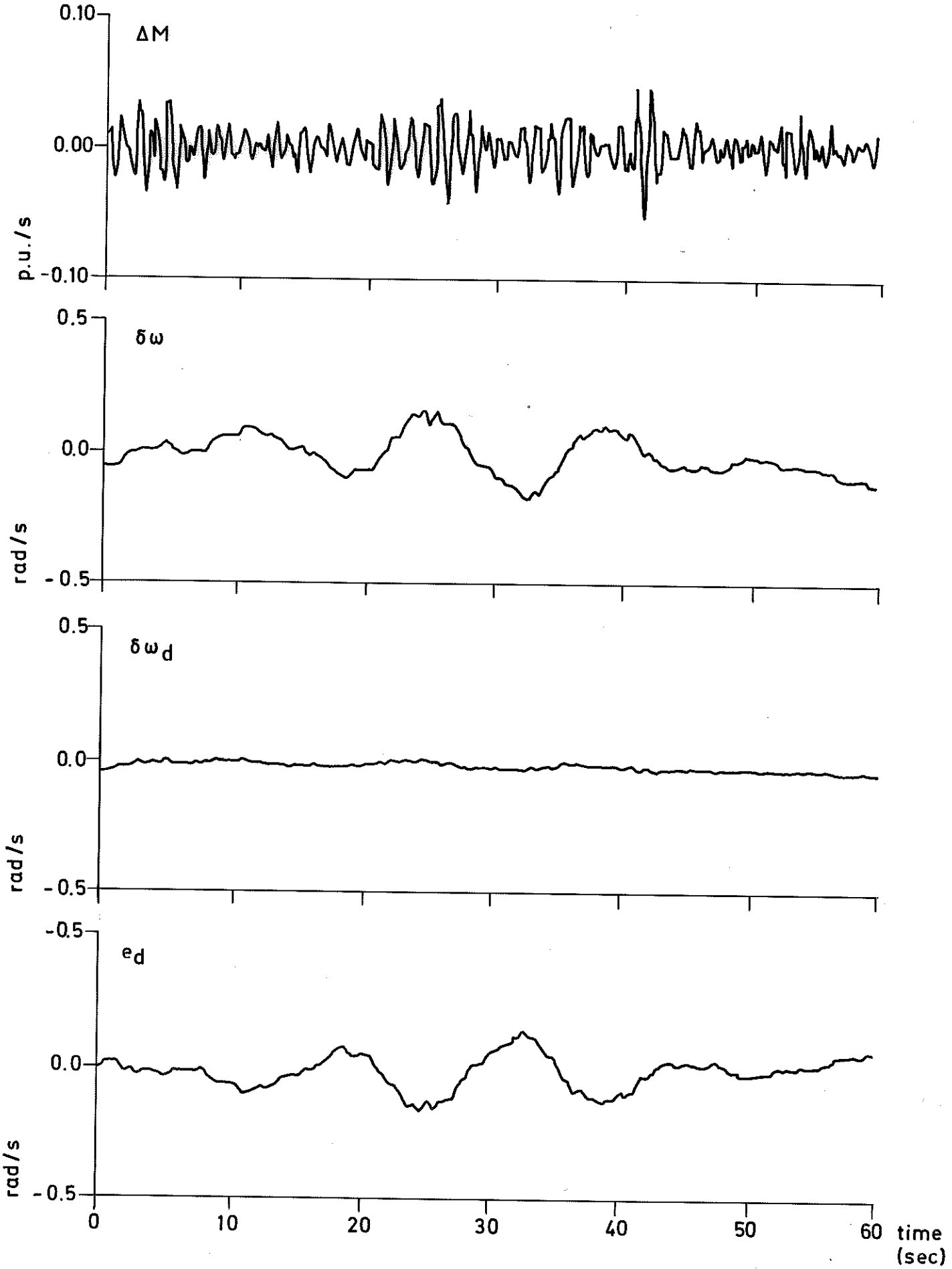

Fig. 6.2. Time responses for the second order state space model (6.12), (6.13).

7. MAXIMUM LIKELIHOOD IDENTIFICATION

In this section we apply maximum likelihood identification to the problem of determining $G_{M\omega}(s)$, relating electric torque to frequency. Since the identification method is described elsewhere [11], [12], [13], the details are not given here. However, a short summary is presented.

7.1. Outline of the Maximum Likelihood identification method

We assume that the discrete-time version of (2.32) can be described by

$$A^*(q^{-1})y(k) = B^*(q^{-1})u(k) + \lambda C^*(q^{-1})e(k) \qquad (7.1)$$

where

$\{u(k), k=1,2,\ldots,N\}$ is the input

$\{y(k), k=1,2,\ldots,N\}$ is the output

and

$\{e(k), k=1,2,\ldots,N\}$ is a sequence of independent normal (0,1) random variables. We have also introduced the forward shift operator q defined by

$$qx(k) = x(k+1)$$

and the polynomials

$$A(q) = q^n + a_1 q^{n-1} + \ldots + a_n$$
$$B(q) = b_1 q^{n-1} + \ldots + b_n \qquad (7.2)$$
$$C(q) = q^n + c_1 q^{n-1} + \ldots + c_n$$

and the corresponding reciprocal polynomials

$$A^*(q) = q^n A(q^{-1})$$
$$B^*(q) = q^n B(q^{-1}) \qquad (7.3)$$
$$C^*(q) = q^n C(q^{-1})$$

The parameters of (6.1) can be determined using the method of maximum likelihood. The likelihood function L is given by

$$-\log L(\theta,\lambda) = \frac{1}{2\lambda^2} \sum_{k=1}^{N} \varepsilon^2(k) + N \log \lambda + \frac{N}{2} \log 2\pi \qquad (7.4)$$

where

$$C^*(q^{-1})\varepsilon(k) = A^*(q^{-1})y(k) - B^*(q^{-1})u(k) \qquad (7.5)$$

where u is the applied input and y is the output. The likelihood function is considered as a function of θ and λ where θ is a vector whose components are the parameters

$$a_1, a_2, \ldots, a_n, b_1, b_2, \ldots, b_n, c_1, c_2, \ldots, c_n, d_1, d_2, \ldots, d_n$$

where $d_1, d_2, \ldots, d_n$ are the n initial conditions of (7.5). The identification problem is then reduced to a problem of minimizing a function of several variables. The maximum

likelihood estimate is consistent, asymptotically normal and efficient under mild conditions given in [14]. Maximizing the likelihood function is equivalent to minimizing the loss function

$$V(\Theta) = \frac{1}{2} \sum_{k=1}^{N} \varepsilon^2(k) \qquad (7.6)$$

where the residuals $\varepsilon(k)$ are obtained from (7.5).

As the order of the model is seldom known apriori we repeate the identification for increasing order of the model and test if the loss function (6.6) is significantly reduced. Now let V_n denote the minimal value of the loss function for the n-th order model. We use the following test quantity

$$t_{n\ n+k} = \frac{V_n - V_{n+k}}{V_{n+k}} \quad \frac{N-4(n+k)}{4k}$$

which has a F(4k, N-4(n+k)) distribution under the null hypothesis. When N is large $t_{n+k,n}$ tends to a χ^2 distribution with 4k degrees of freedom. Most often the test is used with k=1, that is we test the model of order n+1 against the model of order n. It is used at a risk level of 5 %, that is if the test quantity is greater than than 2.37 (N is supposed to be larger than 100) the loss function has been reduced significantly and the order of the model is at least n+1.

7.2. Result of the Maximum Likelihood Identification, δM-$\delta\omega$-series

The δM-$\delta\omega$-series, previously analyzed in section 6.3, is also analyzed, using the maximum likelihood program. In Table 7.1 the estimated values of the parameters are given together with the estimated standard deviation of the parameters. Furthermore the estimated value of λ and the minimal loss function, V_n, for each model are given. The test quantities $t_{n-1,n}$ are also given.

In Table 7.2 we give the zeroes of the polynomials A, B and C.

When we increase the model order from five to six, the loss function is not reduced significantly. When we increase the model order from five to seven the test quantity is 2.43. Thus we conclude that five is the lowest order of the model we can accept.

n	i	$\hat{a}_i \pm \sigma(\hat{a}_i)$	$\hat{b}_i \pm \sigma(\hat{b}_i)$	$\hat{c}_i \pm \sigma(\hat{c}_i)$	$\hat{d}_i$	$1000\hat{\lambda}_n$	$1000V_n$	$t_{n,n+1}$
1	1	-0.997±0.002	-0.868±0.069	0.848±0.017	-0.043	3.797	7.210	126.0
2	1	-1.611±0.026	-0.283±0.075	0.056±0.025	-0.045	3.092	4.781	26.0
	2	0.616±0.026	-0.180±0.079	0.610±0.037	0.027			
3	1	-2.446±0.032	-0.346±0.075	-0.883±0.028	-0.045	2.941	4.325	73.7
	2	1.900±0.063	-0.052±0.141	0.489±0.049	0.065			
	3	-0.452±0.032	0.396±0.080	-0.569±0.041	-0.022			
4	1	-1.901±0.031	-0.619±0.097	-0.072±0.032	-0.044	2.560	3.328	16.7
	2	0.867±0.059	0.536±0.191	-0.066±0.028	-0.038			
	3	-1.781±0.056	-0.698±0.189	-0.077±0.026	0.001			
	4	0.053±0.028	0.776±0.098	-0.673±0.024	0.000			

Table 7.1. Maximum Likelihood Estimates of the parameters in the discrete model (7.1).

Cont.

5	1	-2.628±0.031	-0.835±0.092	-0.899±0.036	-0.046	2.496	3.115	2.03
	2	2.290±0.074	1.120±0.244	-0.005±0.039	0.069			
	3	-0.715±0.082	-0.805±0.308	-0.013±0.036	-0.029			
	4	0.078±0.067	0.599±0.250	-0.624±0.034	0.000			
	5	-0.025±0.026	-0.080±0.100	0.579±0.029	0.002			
6	1	-1.945±0.035	-0.849±0.098	-0.209±0.044	-0.047	2.486	3.090	5.66
	2	0.509±0.071	0.589±0.203	-0.609±0.042	0.038			
	3	0.706±0.067	-0.079±0.201	-0.103±0.041	0.018			
	4	-0.061±0.062	0.113±0.205	-0.541±0.037	-0.014			
	5	-0.297±0.060	0.254±0.206	0.150±0.039	-0.006			
	6	0.089±0.029	-0.032±0.113	0.381±0.035	0.004			

n	A-polynomial		B-polynomial		C-polynomial	
	Real part	Im. part	Real part	Im.part	Real part	Im.part
1	0.997	0.000			-0.848	0.000
2	0.624	0.000	0.634	0.000	-0.028	0.781
	0.986	0.000			-0.028	-0.781
3	0.457	0.000	-0.075	1.620	-0.047	0.761
	0.995	0.035	-0.075	-1.620	-0.047	-0.761
	0.995	-0.035			0.978	0.000
4	-0.045	0.227	-0.056	0.956	-0.883	0.000
	-0.045	-0.227	-0.056	-0.956	-0.006	0.888
	0.995	0.037	0.978	0.000	-0.006	-0.888
	0.995	-0.037			0.967	0.000
5	-0.007	0.195	0.157	0.000	-0.891	0.000
	-0.007	-0.195	0.033	0.583	-0.006	0.894
	0.650	0.000	0.033	-0.583	-0.006	-0.894
	0.994	0.030	1.119	0.000	0.901	0.037
	0.994	-0.030			0.901	-0.037
6	-0.513	0.332	-0.611	0.000	-0.773	0.107
	-0.513	-0.332	0.078	0.778	-0.773	-0.107
	0.465	0.000	0.078	-0.778	-0.025	0.876
	0.517	0.000	0.119	0.000	-0.025	-0.876
	0.994	0.031	1.031	0.000	0.902	0.051
	0.994	0.031			0.902	-0.051

Table 7.2. Zeroes of the polynomials in the discrete model (7.1)

In Fig. 7.1 we show show the input, δM_e and in Fig. 7.2 and 7.3 we show the result of the identification for the first and fifth order models. In Fig. 7.2 and 7.3 we show

a) the output, $\delta\omega$

b) the deterministic model output, $\delta\omega_d$

c) the deterministic model error, $e_d = \delta\omega - \delta\omega_d$

d) the residuals, ω

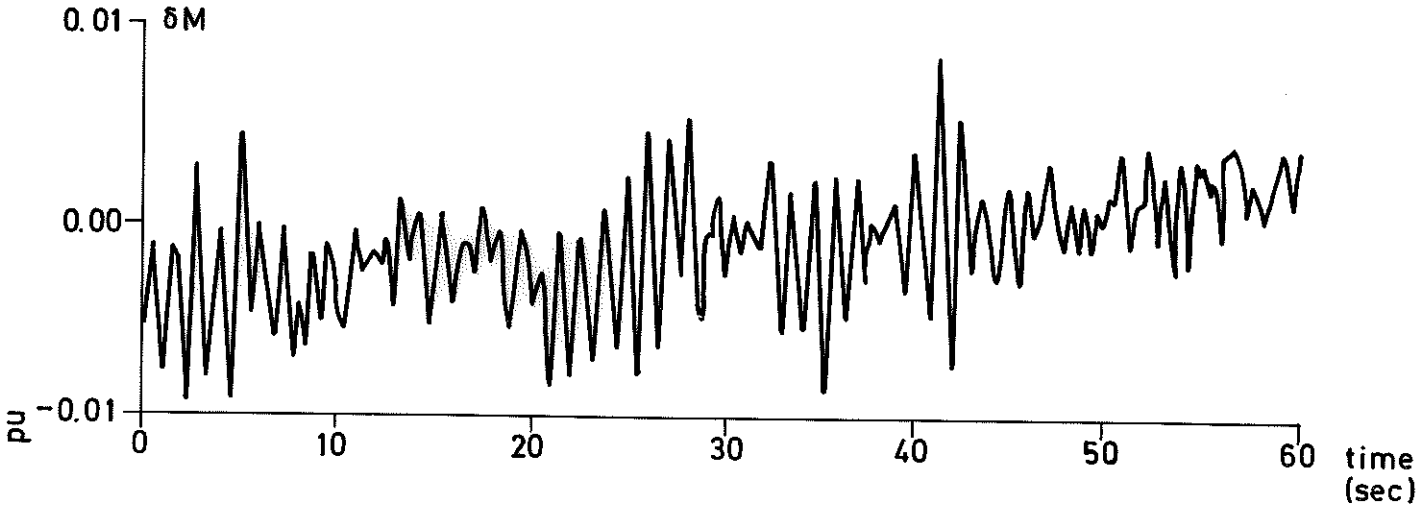

Fig. 7.1. The input signal, δM

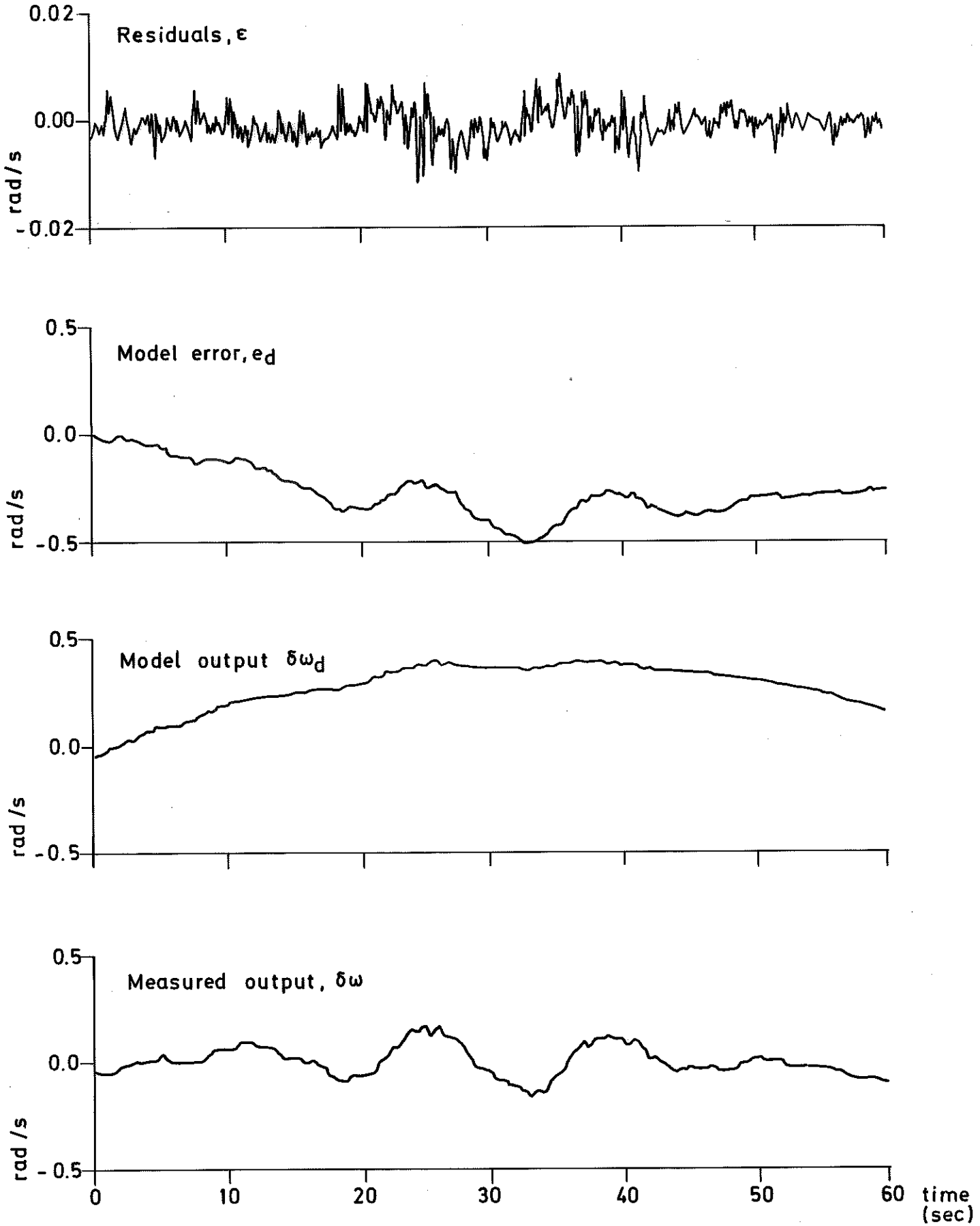

Fig. 7.2. Result of ML-identification, δM-δω-series (first order model)

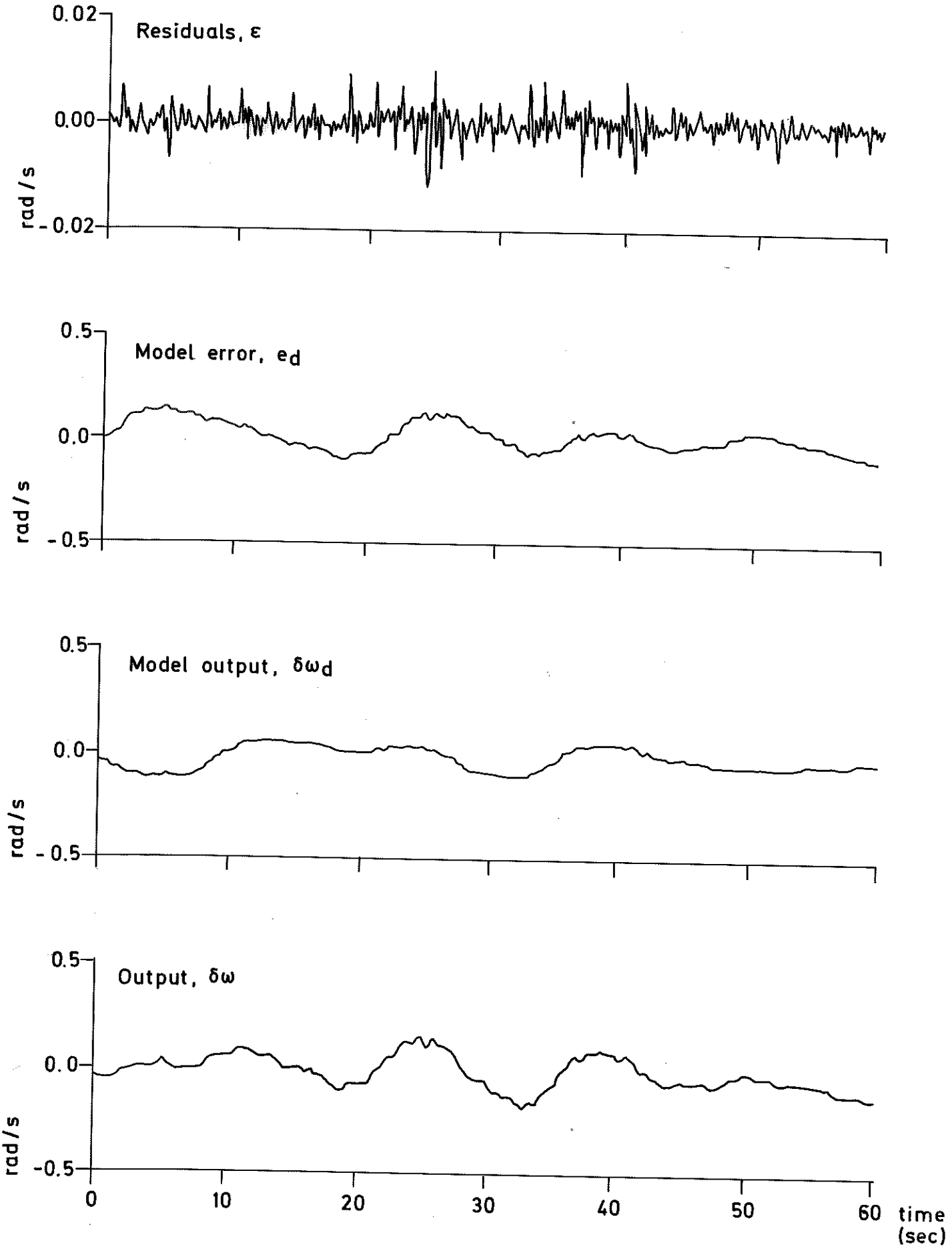

Fig. 7.3. Result of ML-identification, δM-δω-series (fifth order model)

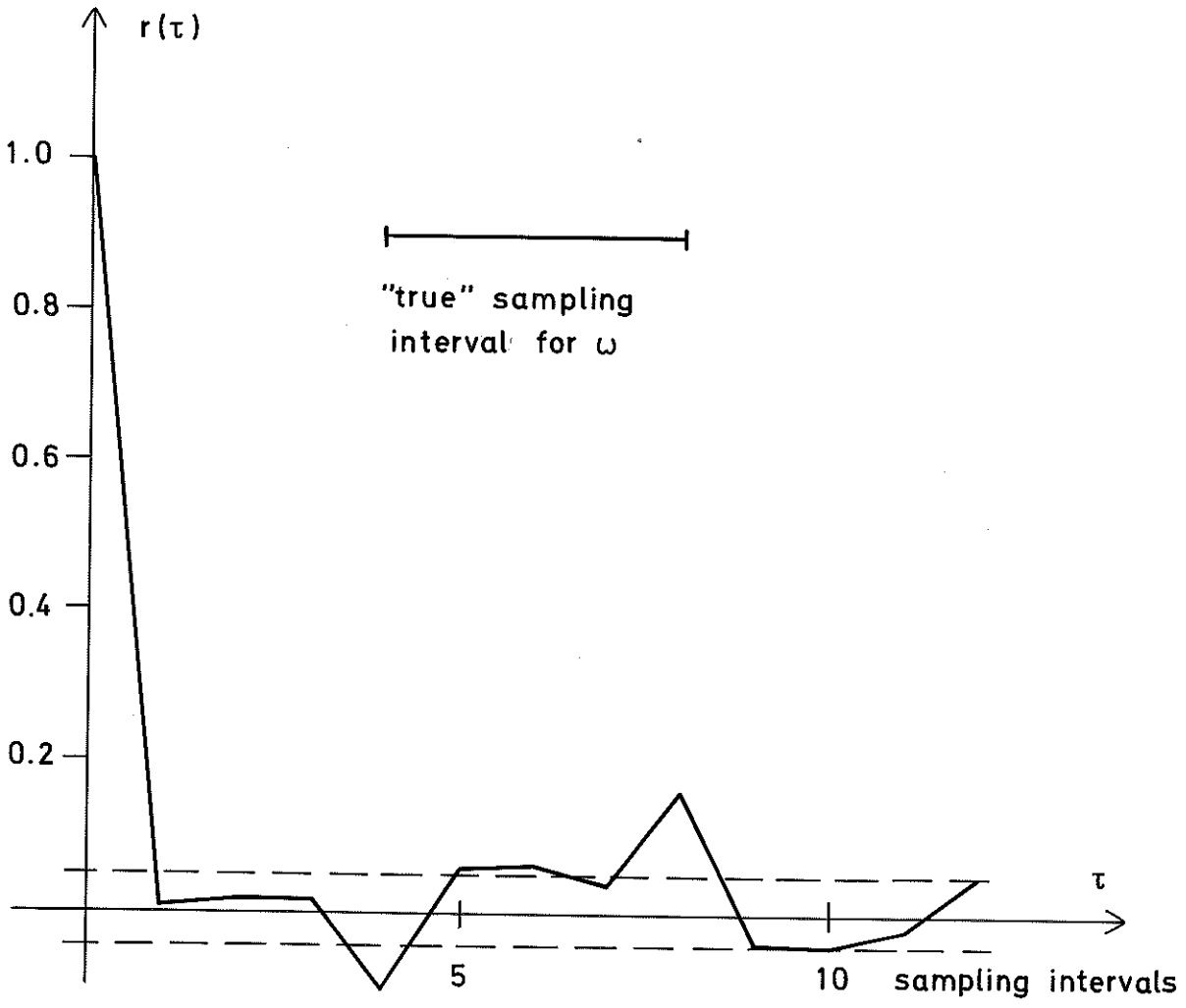

Fig. 7.4. Sample covariance $r(\tau)$ for the residuals of the model (7.1) with n=5. The dashed lines give the 5 % confidence interval for $r(\tau), \tau \neq 0$.

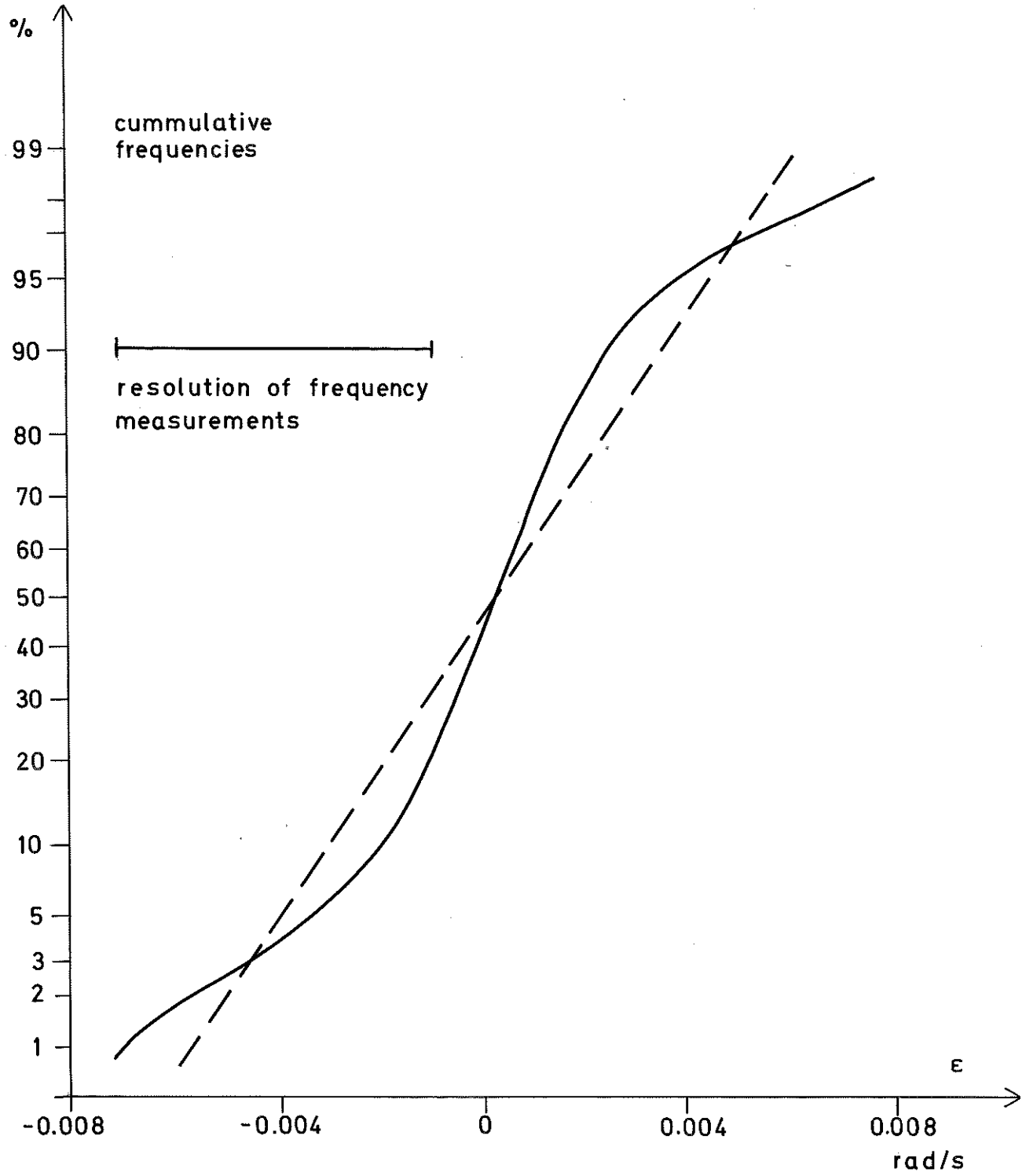

Fig. 7.5. Test of normality of the residuals of the model (7.1) with n=5.

The residuals are assumed to be normal and uncorrelated. To test if this assumption is valid we have computed the auto-correlation function. If the residuals are independent the auto-correlation function should equal zero for $\tau \neq 0$. In Fig. 7.4 the auto-correlation function for the residuals of the fifth order model are shown. We observe the pronounced peak of the auto-correlation function for $\tau = 4$ and $\tau = 8$. Remember that ω is measured only at every fourth point and interpolated at the points between.

The Chi-Square Goodness-of-Fit Test (CSGFT) shows that the residuals are not normally distributed. The explanation is the large discretization error in the measurements of ω (at least when they are compared with the variance of the residuals). In Fig. 7.5 we show the cummulative frequencies for the residuals. The cummulative frequencies for a normal process with the same variance equals the dashed line in Fig. 7.5.

8. ESTIMATION OF PARAMETERS IN A FIFTH ORDER STATE SPACE MODEL

In section 6 we saw that a first order model could explain only a minor part of the output signal. The maximum likelihood identification in section 7 indicated a fifth order model relating angular velocity to electrical torque. We also observed that the eigenvalues of the model were located near the unit circle. indicating that the sampling interval (0.125 sec) was short compared with the time constants of the dominating modes. The sampling interval, however, was so long that ψ_d and ψ_q assumed their final value after a time much shorter than the sampling interval.

When estimating parameters in a fifth order model we used a sampling interval of 0.5 sec, to avoid interpolation in the ω-sequence. This means that we use only measured ω-values.

To eliminate part of the high-frequence disturbances we use the mean value of four consecutive samples as the measured value for the other variables.

8.1. The Fifth Order Nonlinear Model

When modeling the generator we neglect $d\psi_d/dt$- and $d\psi_q/dt$-terms in the expressions for induced voltages. We also want to include a simple model of the environment and

assume that the generator is connected to the network via a lossless line. It is also assumed that the network can be represented by an equivalent generator with constant terminal voltage. The differential equations now become:

$$\frac{d\theta_1}{dt} = \omega_1 - \omega_o \tag{8.1}$$

$$\frac{d\omega_1}{dt} = \left[P_{m1}/\omega_1 - M_{e1} - D(\omega_1-\omega_2)\right] /J \tag{8.2}$$

$$\frac{d\psi_f}{dt} = v_f - i_f r_f \tag{8.3}$$

$$\frac{d\theta_2}{dt} = \omega_2 - \omega_o \tag{8.4}$$

$$\frac{d\omega_2}{dt} = \left[P_{m2}/\omega_2 - M_{e2} - D(\omega_2-\omega_1)\right] /J_2 \tag{8.5}$$

The equations relating the measured variables to the states are:

$$y_1 = \omega_1 \tag{8.6}$$

$$y_2 = \sqrt{v_d^2 + v_q^2} \tag{8.7}$$

$$y_3 = \cos\delta\, i_d - \sin\delta\, i_q \tag{8.8}$$

$$y_4 = \sin\delta\, i_d + \cos\delta\, i_q \tag{8.9}$$

The following algebraic relations shall also be satisfied:

$$M_{e1} = \psi_d i_q - \psi_q i_d \tag{8.10}$$

$$P_d = \omega_2 M_{e2} + \omega_1 M_{e1} - r_a(i_d^2 + i_q^2) \tag{8.11}$$

$$\psi_f = L_{ff} i_f - L_{af} i_d \tag{8.12}$$

$$\psi_d = L_{af} i_f - L_d i_d \tag{8.13}$$

$$\psi_q = - L_q i_q \tag{8.14}$$

$$tg\ \delta = v_d / v_q \tag{8.15}$$

$$\omega_1 \psi_d = v_q + r_a i_q \tag{8.16}$$

$$\omega_1 \psi_q = -v_d - r_a i_d \tag{8.17}$$

$$v_d = v_b \sin(\theta_1 - \theta_2) - X_\ell i_q \tag{8.18}$$

$$v_q = v_b \cos(\theta_1 - \theta_2) - X_\ell i_d \tag{8.19}$$

The angle between a fixed point on the rotor and the standard time phasor is denoted by θ_1. The rate of change of the rotor angle θ_1 is denoted by ω_1. Equation (8.2) is a torque balance for the rotor. The mechanical power delivered from the turbine to the generator is denoted by P_{m1}. The airgap torque is denoted by M_{e1} and $D(\omega_1 - \omega_2)$ represents the damping torque. Equation (8.3) is obtained from the

induction law applied on the field circuit. The field voltage. current and resistance are denoted by v_f, i_f and r_f respectively. The angle between a fixed point on the rotor of the generator, representing the network. and the standard timephasor is denoted by θ_2, while ω_2 is the rate of change of θ_2. Equation (8.5) is a torque balance for the equivalent generator.

The output signals are the angular velocity of the rotor ω_1, the terminal voltage v_t, the reactive current I_q and the active current I_r.

The expression for the air gap torque (8.10) was also given in section 2. Equation (8.11) reflects the assumption that the transmission line i lossless. The flux linkages are given by equation (8.14). The angle between the quadrative axis and the terminal voltage is denoted by δ and equation (8.15) is obtained from a phasor diagram. Application of the induction law on the stator winding and neglecting the $d\psi_d/dt$- and $d\psi_q/dt$-terms gives equation (8.6) and (8.17).

Equation (8.18) and (8.19) are obtained from a phasor diagram.

Collecting equation (8.1) to (8.5) and (8.10) to (8.19) we have:

$$f(\dot{v},v) = 0 \tag{8.20}$$

Equation (8.6) to (8.9) can be collected to:

$$g(y,v) = 0 \tag{.21}$$

8.2. Derivation of the fifth order linear state space model

Having obtained the nonlinear model (8.20) and (8.21) we are now faced with the problem of deriving the linear state space model. The steady-state values are obtained if we put time derivatives equal to zero in equation (8.20) and (8.21) viz.

$$f(0.\bar{v}) = 0 \tag{8.22}$$

$$g(\bar{y},\bar{v}) = 0 \tag{8.23}$$

The zero solution of the nonlinear equation (8.22) and (8.23) can be obtained by standard techniques, e.g. Newton-Raphson method but we exploit the special structure of the problem.

After linearization equation (8.20) and (8.21) can be written

$$E\dot{v} + Fv = 0 \tag{8.24}$$

$$Py + Qv = 0 \tag{8.25}$$

where

$$E = f_v(0,\bar{v})$$

$$F = f_v(0,\bar{v})$$

$$P = g_y(\bar{y},\bar{v})$$

$$Q = g_v(\bar{y},\bar{v})$$

To avoid new symbols the perturbed variables, that are the differences $v-\bar{v}$ and $y-\bar{y}$ are denoted by v and y.

Having obtained the matrices E, F, P and Q in (8.24) and (8.25) we use a model building program (RESTAF), described in [15] to obtain the linear state space equations

$$\frac{dx}{dt} = Ax \tag{8.26}$$

$$y = Cx \tag{8.27}$$

After transformation to discrete time we have

$$x(t+T) = \Phi x(t) \tag{8.28}$$

$$y(t) = Cx(t) \tag{8.29}$$

where

$$\Phi = e^{AT}$$

Equation (8.28) and (8.29) represents the deterministic part of the linear stochastic system

$$\hat{x}(t+T) = \Phi\hat{x}(t) + K\varepsilon(t) \tag{8.30}$$

$$y(t) = C\hat{x}(t) + \varepsilon(t) \tag{8.31}$$

where $\{\varepsilon(t)\}$ is a sequence of independent equally distributed gaussian vectors with zero mean and covariance R.

The state variable x of (8.30) and (8.31) can be interpreted as the best linear estimate of the state x of (8.28) and (8.29) based on observed outputs. The matrix K can be interpreted as the steady state gain of the Kalman filter associated with the model (8.28) and (8.29).

This is a nice property since implementation of a Kalman filter for reconstruction then requires no additional compuation.

8.3. Choice of Parameters

A canonical representation of the model (8.30), (8.31) will, in this case, contain 50 unknown parameters which give an upper bound on the number of parameters in an

identifiable model [9].

Since nothing is known about the matrix K, there are at least 20 parameters to be identified. The problem is then to find a set of parameters which give an identifiable model and where the fixed parameters of A and C do not essentially restrict the input-output relations defined by the model. It is also important (computational aspects) that the number of unknown parameters is as small as possible.

The deterministic part of the model is defined by ten parameters which means a total number of 30 parameters. An attempt was made to estimate all 30 parameters but unrealistic values of r_a and r_f was obtained. It was then decided not to include r_a and r_f in the parameter vector.

8.4. Result of the Identification

The final choice of parameters, which gave realistic values of the parameters, is shown in table 8.1. The inclusion of r_a and r_f in the parameter vector gave only a small improvement of the loss function V. The value of the loss function has been decreased from $0.8\ 10^{-6}$ to $0.145\ 10^{-10}$ by the identification. Parameters J_1, J_2 and X_ℓ have been subjected to the largest changes.

The initial value of J_1 is in the neighbourhood of the value obtained in Section 6 and the initial value of J_2 is chosen to be one order of magnitude larger than J_1. The estimated value of J_1 differs from the value quoted by the manufacturer by a factor 2.5. The estimated value of J_2 is still one order of magnitude larger than the value of J_1. It is not surprising that the initial guess of X_ℓ, which is part of the model of the environment, has been subjected to a large change. The values of X_{ff}, X_{af}, X_d and X_q are all realistic. Saturation in the magnetic circuits may be the explanation to the fact that the estimated value of X_q is larger than the estimated value of X_d.

	Initial	Estimated
J_1	0.22	0.00872
J_2	5.0	0.121
D	0.01	0.0051
X_ℓ	0.1	1.112
X_{ff}	2.0	2.36
X_{af}	1.2	1.341
X_d	1.0	0.846
X_q	0.8	0.888
k_{11}	0.0	0.00530
k_{12}	0.0	-1.147
k_{13}	0.0	-0.222
k_{14}	0.0	-0.0633
k_{21}	0.0	1.201
k_{22}	0.0	0.388
k_{23}	0.0	0.0159
k_{24}	0.0	-0.0162
k_{31}	0.0	-0.000012
k_{32}	0.0	0.0081
k_{33}	0.0	0.00177
k_{34}	0.0	0.000527
k_{41}	0.0	0.00521
k_{42}	0.0	1.417
k_{43}	0.0	0.160
k_{44}	0.0	0.0320
k_{51}	0.0	1.205
k_{52}	0.0	-0.0576
k_{53}	0.0	0.0161
k_{54}	0.0	0.00939

Table 8.1. Initial and estimated parameters of the model (8.30), (8.31).

	Initial	Estimated
J_1	0.22	0.00872
J_2	5.0	0.121
D	0.01	0.0051
X_ℓ	0.1	1.112
X_{ff}	2.0	2.36
X_{af}	1.2	1.341
X_d	1.0	0.846
X_q	0.8	0.888
k_{11}	0.0	0.00530
k_{12}	0.0	-1.147
k_{13}	0.0	-0.222
k_{14}	0.0	-0.0633
k_{21}	0.0	1.201
k_{22}	0.0	0.388
k_{23}	0.0	0.0159
k_{24}	0.0	-0.0162
k_{31}	0.0	-0.000012
k_{32}	0.0	0.0081
k_{33}	0.0	0.00177
k_{34}	0.0	0.000527
k_{41}	0.0	0.00521
k_{42}	0.0	1.417
k_{43}	0.0	0.160
k_{44}	0.0	0.0320
k_{51}	0.0	1.205
k_{52}	0.0	-0.0576
k_{53}	0.0	0.0161
k_{54}	0.0	0.00939

Table 8.1. Initial and estimated parameters of the model

The estimated covariance matrix $\hat{R}$ equals

$$\hat{R} = \begin{bmatrix} 0.602 \cdot 10^{-3} & 0.121 \cdot 10^{-5} & 0.937 \cdot 10^{-5} & -0.241 \cdot 10^{-4} \\ 0.121 \cdot 10^{-5} & 0.231 \cdot 10^{-6} & -0.843 \cdot 10^{-6} & -0.233 \cdot 10^{-6} \\ 0.937 \cdot 10^{-5} & -0.843 \cdot 10^{-6} & 0.441 \cdot 10^{-5} & -0.145 \cdot 10^{-5} \\ -0.241 \cdot 10^{-4} & -0.233 \cdot 10^{-6} & -0.145 \cdot 10^{-5} & 0.590 \cdot 10^{-5} \end{bmatrix}$$

The standard deviations of the one-step ahead prediction error then are

$\sigma_{\varepsilon_1} = 0.246 \cdot 10^{-1}$ rad/s

$\sigma_{\varepsilon_2} = 0.488 \cdot 10^{-3}$ p.u.

$\sigma_{\varepsilon_3} = 0.213 \cdot 10^{-2}$ p.u.

$\sigma_{\varepsilon_4} = 0.244 \cdot 10^{-2}$ p.u.

As the model does not have any input signal, it is impossible to show the deterministic model output and the error of the deterministic model. In Fig. 8.1 we show

a) measured output, y

b) model output, y_m

c) residuals, ε

In Fig. 8.2 we show measured output, model output and residuals from simulation on data not used in the identification.

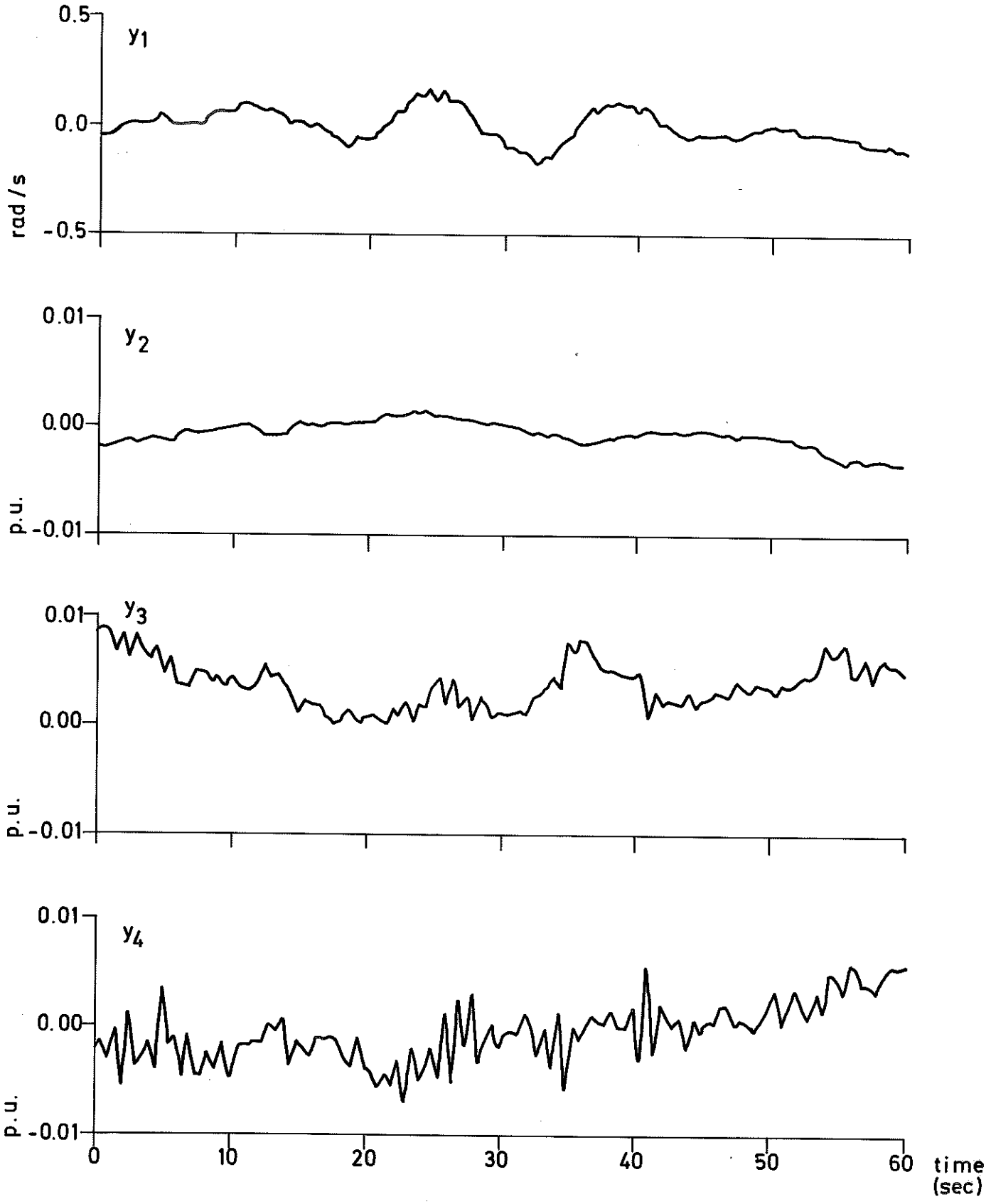

Fig. 8.1.a. Output $y_1(t)$ = angular velcoity, $y_2(t)$ = terminal voltage, $y_3(t)$ = reactive current and $y_4(t)$ = active current of the turbogenerator.

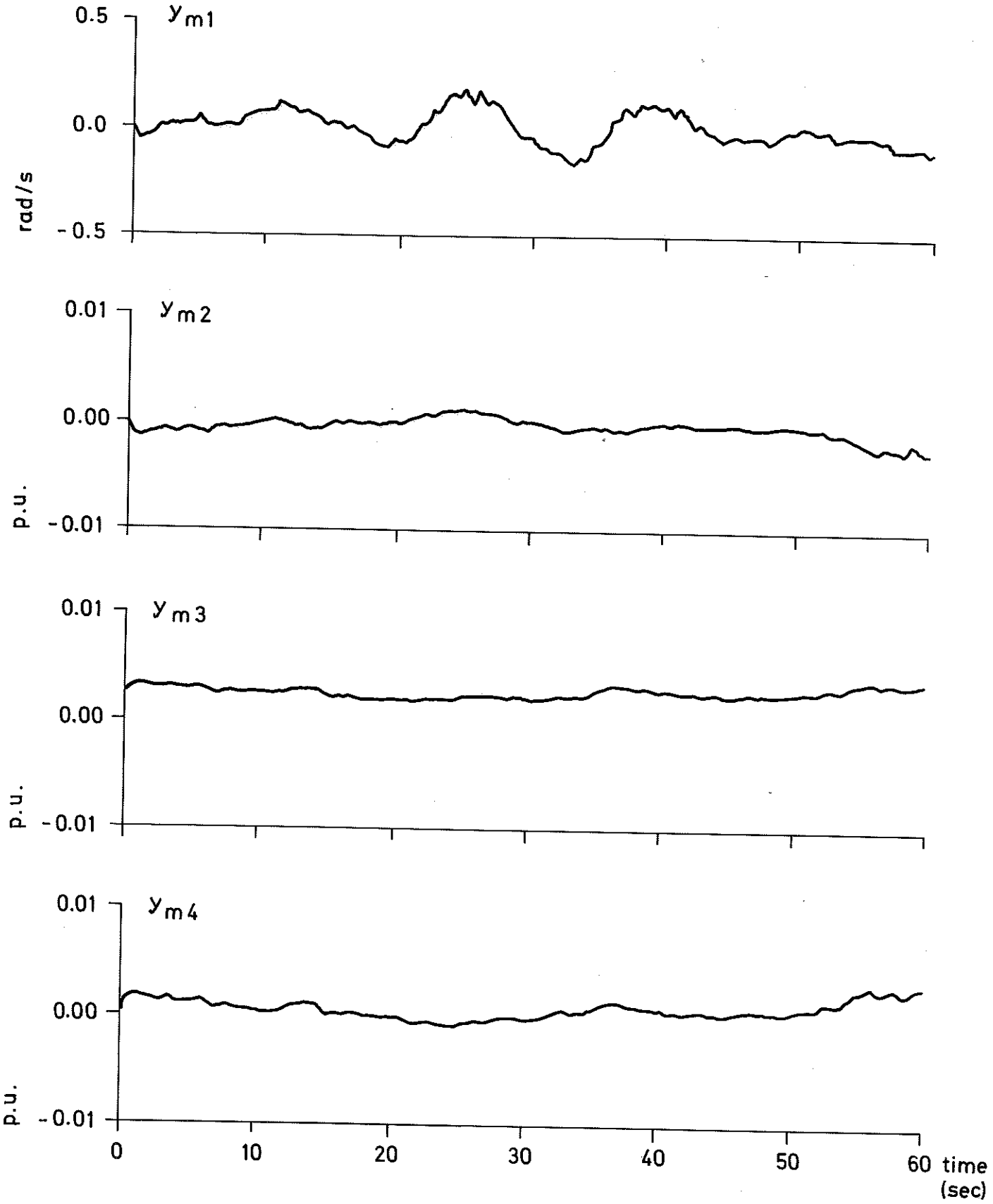

Fig. 8.1.b. Model output $y_{m1}(t)$ = angular velocity, $y_{m2}(t)$ = terminal voltage, $y_{m3}(t)$ = reactive current and $y_{m4}(t)$ = active current of the model (8.30), (8.31). Observe that we show the output of the one step ahead predictor.

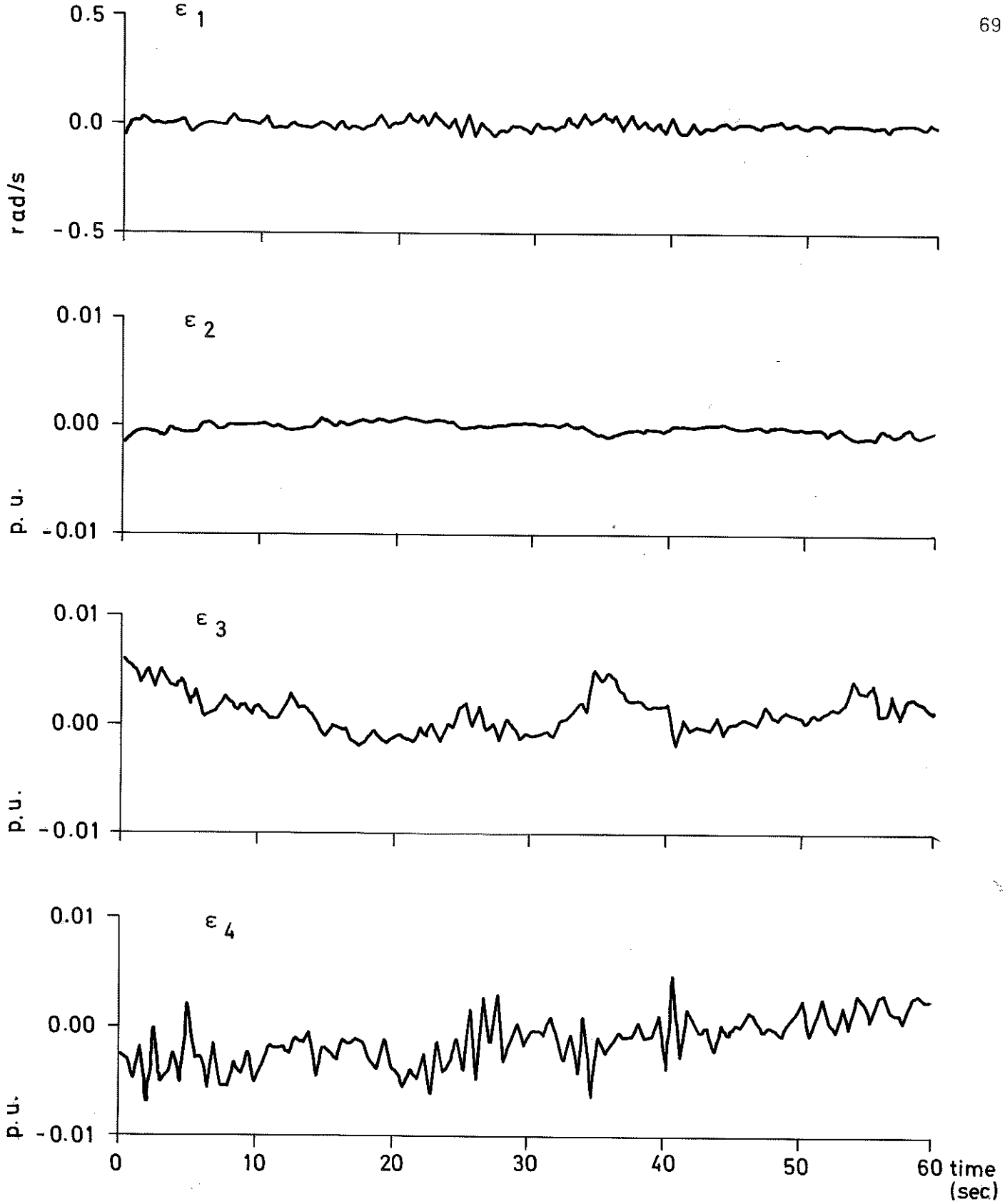

Fig. 8.1.c. Residuals $\varepsilon_1(t)$ of angular frequency, $\varepsilon_2(t)$ of terminal voltage, $\varepsilon_2(t)$ of reactive current and $\varepsilon_y(t)$ of active current of the model (8.30),(8.31). Observe that we show the one step ahead prediction error.

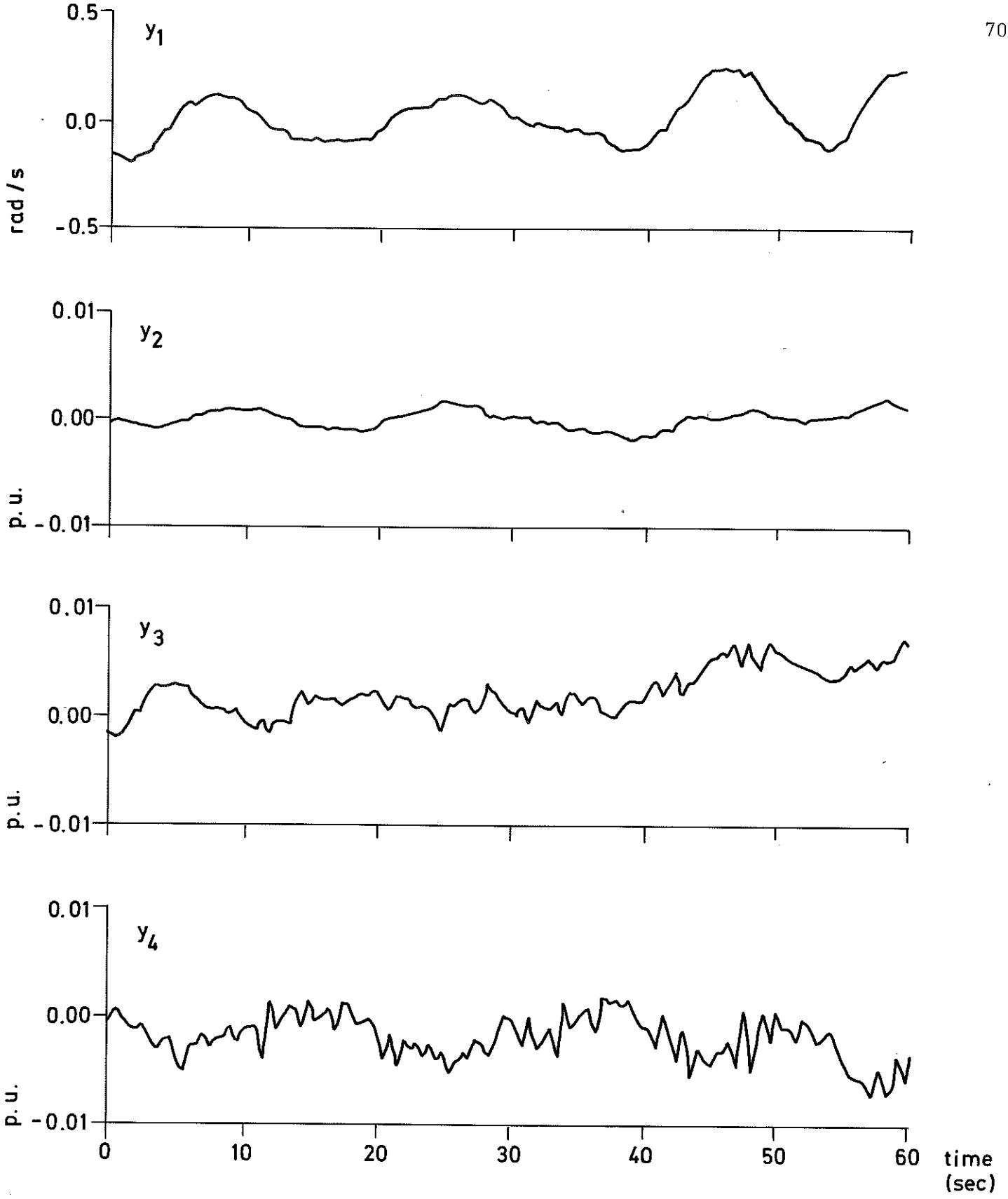

Fig. 8.2.a. Output of the turbo-generator not used in the parameter estimation.

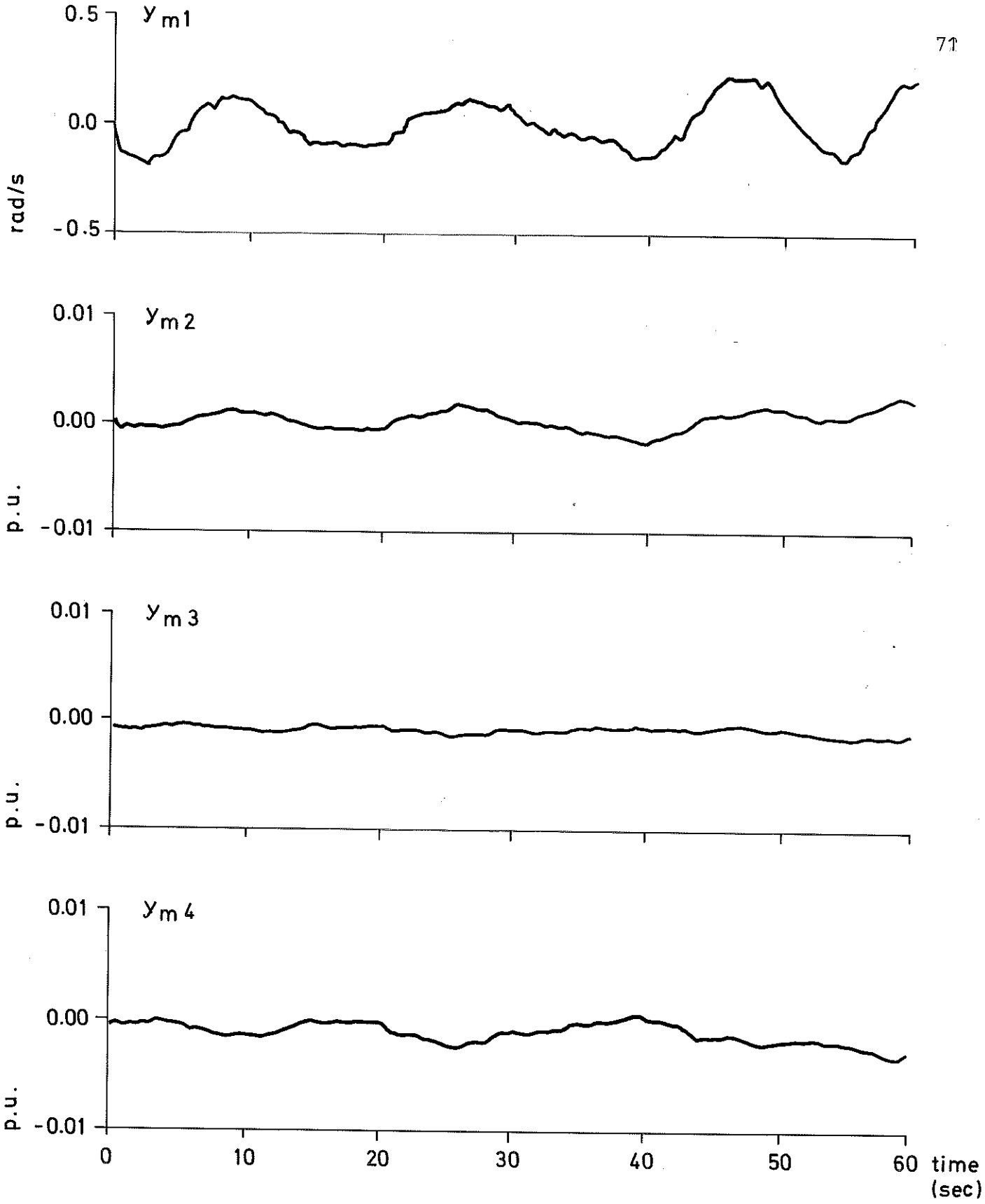

Fig. 8.2.b. Model output from the model (8.30), (8.31) when simulated on data not used in the parameter estimation. Observe that we show the output of the one step ahead predictor.

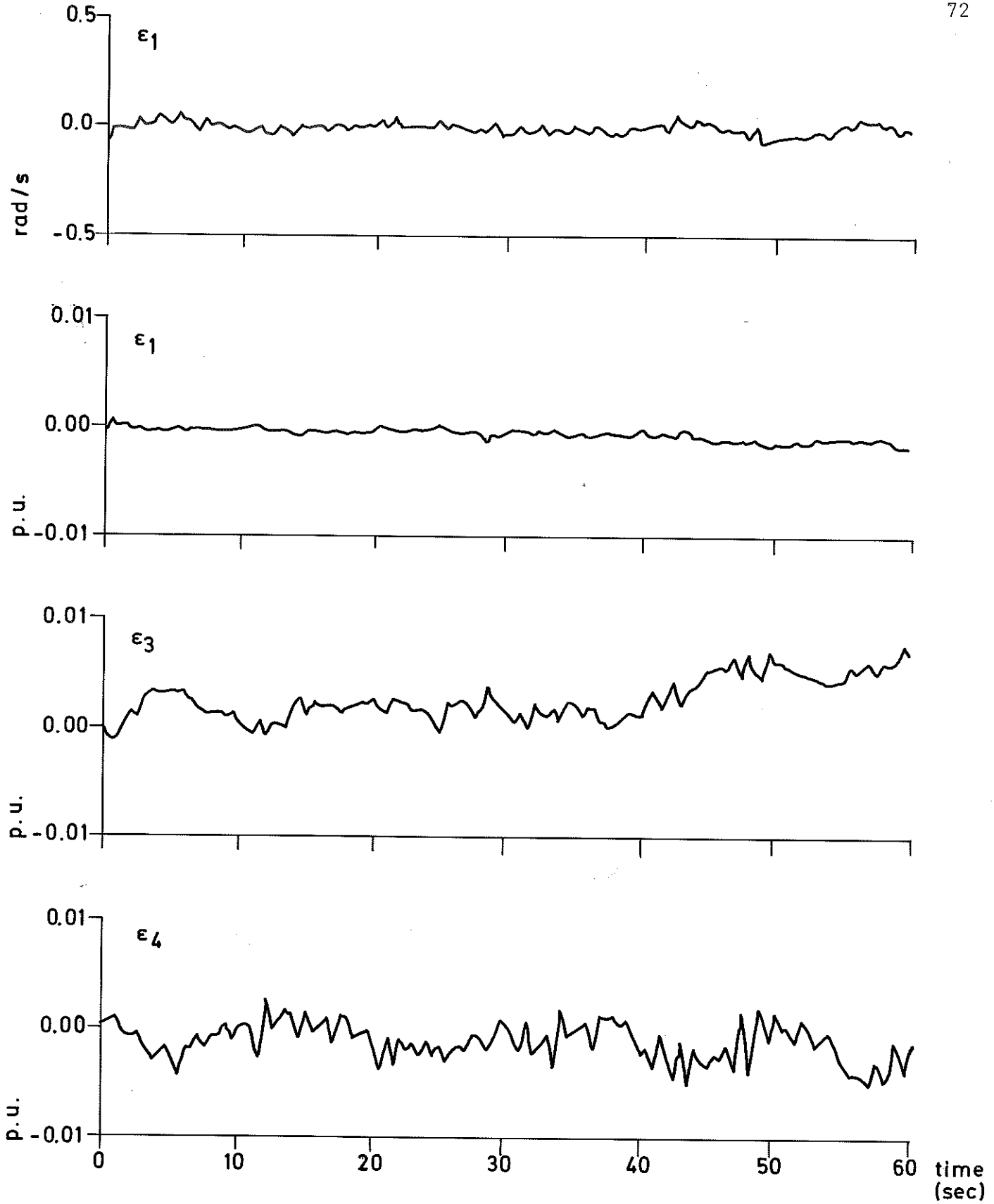

Fig. 8.2.c. Residuals of the model (8.30), (8.31) when simulated on data not used in the parameter estimation. Observe the one step ahead prediction error.

The residuals $\{\varepsilon(t)\}$ should equal a realization of discrete time white noise if the conditions of the identification method are fulfilled and if the minimum is achieved. Fig. 8.3 shows the sample covariance function of $\{\varepsilon_1(t)\}$. The sample covariance function of $\varepsilon_1(t)$ shows that sequence $\varepsilon_1(t)$ differs from a realization of discrete time white noise. The other sample covariance functions look even worse.

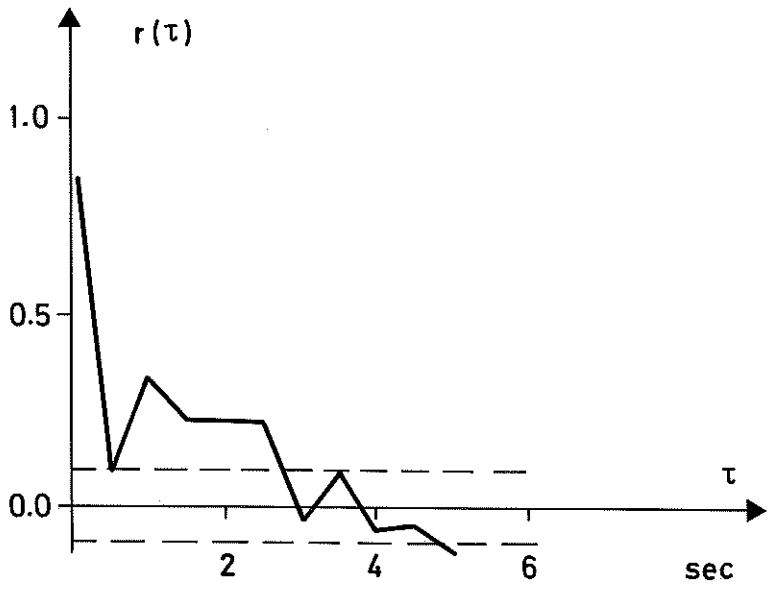

Fig. 8.3. Sample covariance function for the residuals $\{\varepsilon_1(t)\}$ of the model (8.30), (8.31). The dashed lines give the 5 % confidence interval for $r(\tau)$, $\tau \neq 0$.

The minimization could not be done in one run and it was necessary to interfere manually, by choosing different subset of parameters. The minimization of the loss function with respect to one variable took about one minute on the UNIVAC 1108. The identifiability of the model could not be verified.

8.5. Conclusions

In spite of the difficulties encountered with the minimization algorithm it is not believed possible to obtain significantly better models without using new experiments. When performing such experiments it is desirable to introduce artificial disturbances, i.e. pseudo-random binary signals (PRBS).

Computing time has turned out to be long even for a moderate number of parameters.

Since this number easily grows, the identification method heavily depends on the minimization algorithm which is used. In the first runs, Stewart's method was used but it proved that further reduction of the loss function was achieved if Powell's method was employed. This implies that no estimate of the matrix of second order derivatives is available.

It is important that the structure of the model is correct. That is, physical phenomena which are important for the

dynamical behaviour must be present in the model. This is the case for the angular velocity and terminal voltage but is not the case for reactive and active current. This depends on the fact that there are significant disturbances from the network in terms of load variations which are not included in the model. In eq. (8.11) the power demand is assumed to be constant with an additive white noise term.

9. CONCLUSIONS

Before we start summing up the conclusions we want to point out that the data used in all sections were collected during normal operation. This means that we in fact try to use data from a closed loop system for the determination of the dynamics of the system. This problem is by no means easy to solve.

In the theoretical analysis of the generator in section 2, the assumption (A2.2) that the stator energy could be neglected was introduced. This assumption enabled us to describe the dynamics from electrical torque to frequency as a first order linear system. In this section we will sum up the results of the previous sections and thereby focus the attention on the validity of such a model. Dr. Stanton has, applying spectral analysis to the same data records, concluded that a first order system well describes the dynamics in question [4].

This result does not seem to be consistent with the results obtained here in section 5 (Fig. 5.3 and 5.4). However, the significance of the estimates is low, and they are subject to the special choice of lag window and the special pre-treatment of data (these were not specified in [4]). The results of section 5, although indicating another conclusion, can therefore not be regarded as opposing to Dr Stanton's results. On the other hand, spectral analysis is not well suited to determine the order of the system for several reasons:

- With noisy data it is quite cumbersome to estimate slopes of the amplitude plot.
- The phase plot could be quite misleading for frequencies over a tenth of the Nyquist frequency.
- The transfer function arrived at will include all feedback effects, also external from the power network. These are not negligable as seen from Fig. 4.4. Hence the estimated transfer function cannot immediately be compared with the theoretical models.

Only a minor part of the frequency variations can be explained with a first order model, whether the torque is assumed to be constant over the sampling interval or the torque is assumed to vary linearly between the samples.

The ML-identification shows that a model of higher order, at least 5, is required to describe the dynamics well. In Fig. 9.1 and 9.2 the fifth order model from the ML-identification is compared with the significant part of the spectral analysis estimate (cf. Fig. 5.5 and 5.6). From these figures it is concluded that, although the agreement is not total, the two methods give results that are consistent. Thus the different identification methods clearly show that higher order models are necessary.

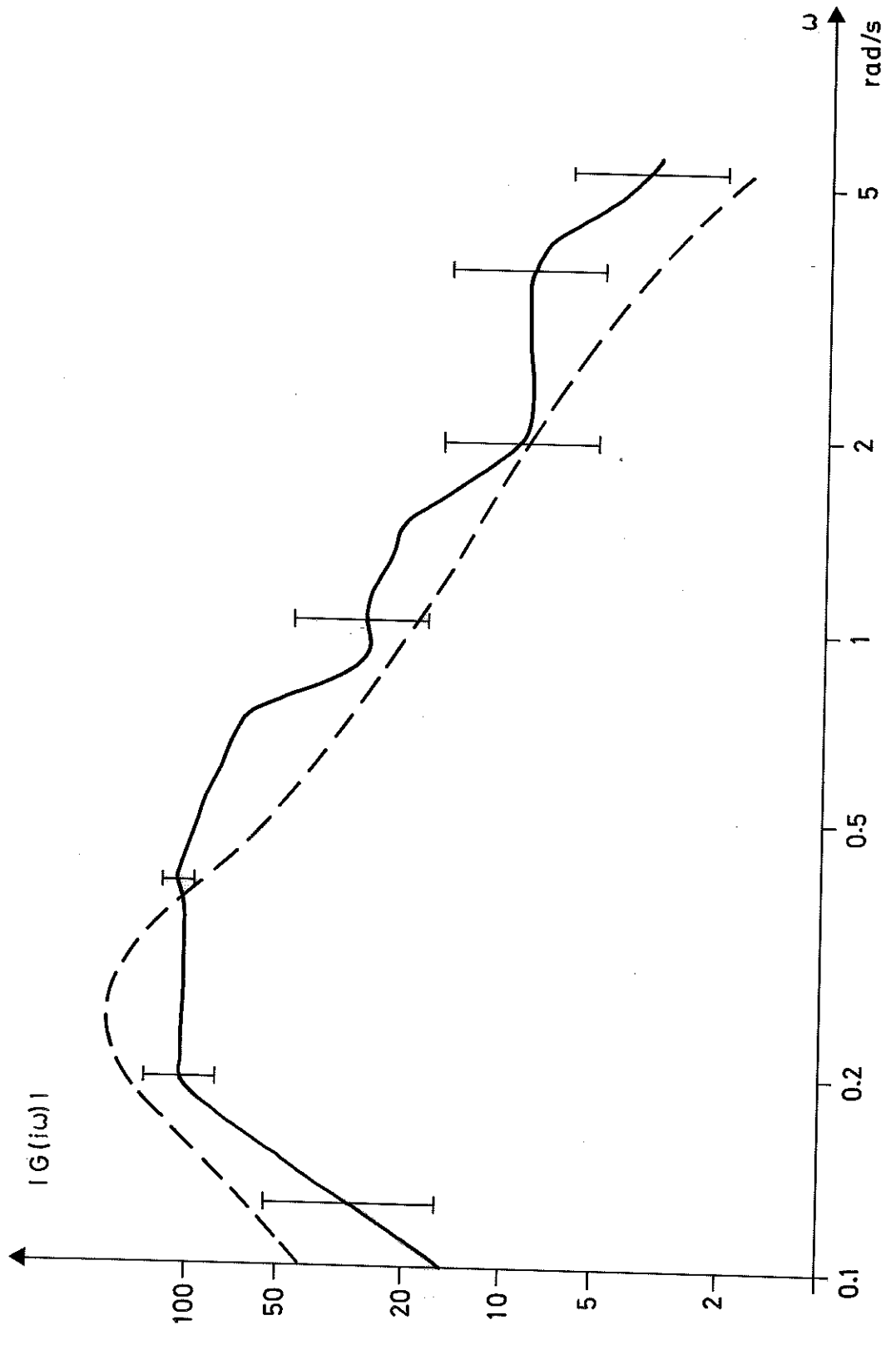

Fig. 9.1. Comparison between amplitude Bode plot, based on the fifth order model from ML-identification (broken) and the result from spectral analysis (solid). Compare Fig. 5.5.

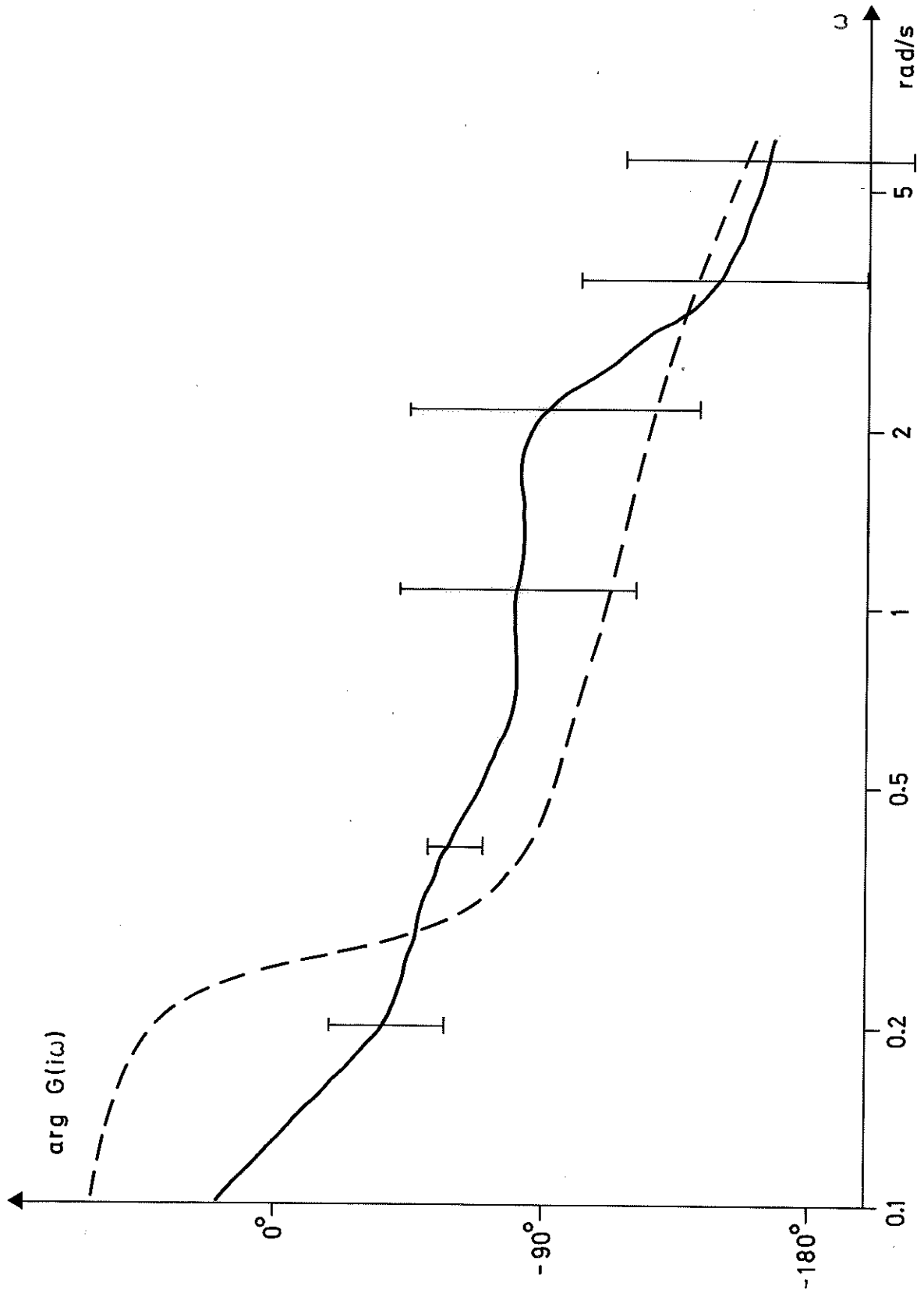

Fig. 9.2. Comparison between phase Bode plot, based on the fifth order model from ML-identification (broken) and the result from spectral analysis (solid). Compare Fig. 5.6.

The fifth order state space model, which was investigated in this paper can reasonably well explain angular velocity and voltage outputs. Some improvements of the model could be obtained if power demand was modeled as output from a low order system, whose input is a white noise process. That means that the following differential equation

$$\frac{dP_d}{dt} = \lambda P_d + e \qquad (9.1)$$

has to be added to the set of differential equations given in Section 8. In eq. (9.1) P_d is the power demand used in eq. (8.11), λ a parameter to identify and e a white noise term.

To obtain still better models new experiments have to be performed. When making such experiments it is desirable to introduce artificial disturbances, i.e. pseudo-random binary sequences (PRBS).

10. REFERENCES

[1] Shackshaft, G., "General-purpose turboalternator model", Proc. I.E.E., Vol. 110, No 4, April 1963, pp 703 - 713.

[2] Park, R.H., "Two-reaction theory of Synchronous Machines; Generalized Methods of Analysis - Part I" Trans. Amer. Inst. Elect. Engrs., 1929, 48, p 716 -

[3] Park, R.H., "Two-reaction theory of Synchronous Machines - II", AIEE Trans., Vol. 52, pp 352 - 355, June 1933.

[4] Stanton, K.N., "Estimation of Turboalternator Transfer Functions using Normal Operating Data", Proc. I.E.E., Vol. 112, 1965, pp 1713 - 1720.

[5] Stanton, K.N., "Use of Normal Operating Data from a Power System to Estimate Turboalternator Transfer Functions" Report,Perdue University, West Lafayette, Indiana.

[6] Stanton, K.N., "An incremental wattmeter for use in interconnected power systems", Elect. Mech. Engng. Trans. Instn. Engrs., Aust., May 1964, p 20.

[7] Ljung, L., "Pilot Estimation of Impulse Response Functions", Preliminary Report, Lund Inst. of Technology, Div. of Automatic Control, 1971.

[8] Jenkins, G.M. & Watts, D.G., "Spectral Analysis and its applications", Holden-Day, San Francisco, 1968.

[9] Åström, K.J. and Eykhoff, P. "System Identification - A Survey", Automatica, Vol. 7, pp 123 - 162

[10] Eaton , J., "Identification for control purposes", Paper IEEE Winter meeting N.Y.

[11] Gustavsson, I., "Parametric Identification of Time Series", Report 6803, Lund Institute of Technology, Division of Automatic Control, April 16, 1968.

[12] Gustavsson, I., "Parametric Identification of Multiple Input Single Output Linear Dynamical Systems", Report 6907, July 1969, Lund Institute of Technology, Division of Automatic Control.

[13] Åström, K.J., and Bohlin, T., "Numerical Identification of Linear Dynamical Systems from Normal Operating Records",in "Theory of Self-Adaptive Systems", P.H. Hammond (ed.) Plenum Press 1966.

[14] Åström, K.J., Bohlin T and Wensmark, S., "Automatic Control of Linear Stochastic Dynamic Models for Stationary Industrial Processes with Random Disturbances using Normal Operating Records", IBM Nordic Laboratory, Sweden, Report TP 18.150.

[15] Eklund, K., "Numerical Modelbuilding", Int. J. Control, 1970, Vol. 11, No 6, 973-985.